

**Glacial Ablation Dynamics and Sediment Flux at Linnébreen,  
Spitsbergen**

Senior Thesis presented

by

Eric P. Helfrich

Department of Geosciences  
University of Massachusetts, Amherst

May 2007

## ABSTRACT

Modern process studies conducted on Arctic glaciers provide valuable insight into dynamic responses observed in the high latitudes due to global scale climate change, with telltale implications for environmental change in the lower latitudes. This research was conducted on Spitsbergen, the largest island of Svalbard, as part of an NSF funded Research Experience for Undergraduates program. The Norwegian High Arctic, containing Svalbard, is influenced by the northern extent of the Gulf Stream and the advection of warm air and moisture to the high latitudes. Its position creates highly variable conditions which directly affect the mass balance of glaciers on Svalbard. Work by Hagen et al. (2003) calculated the surface mass balance of Svalbard to be  $-4.5^{+/-} 1 \text{ km}^3 \text{ yr}^{-1}$ . Understanding the factors influencing glacier mass balance and quantifying ablation rates provides ground-truthed data to gauge the Arctic's reaction to changing climatic conditions and its influence in the global climate system.

A compilation of mass balance measurements, local meteorological data, stream gauge, and suspended sediment concentrations were studied over a five week period during the summer 2006 melt season. High resolution data was collected in 30-minute intervals and manual readings were taken at eight glacier ablation centerline stakes on Linnèbreen. Comparisons were made directly to meteorological data, affording assessment of the correlations between the local and regional weather data and the dynamic behavior of this glacier. Summer precipitation was found to be the main agent of surface lowering on Linnèbreen. Days of high precipitation correlate directly with days of greater surface lowering and peak suspended sediment in the meltwater stream. High rates of lowering are interpreted to be the result of latent heat release caused by meltwater and precipitation percolating down into and refreezing below the glaciers surface. This triggered the removal of overlying ice, providing a glassy surface until such time that eolian debris and new sediment could accumulate and melt in differentially due to contrasts in albedo. Sediment flux to the meltwater stream is derived by erosion of sediment liberated by prior glacial activity. Supply is dominated by active layer thawing around the meltwater stream, resultant of rising temperatures and precipitation induced high discharge. The rise and fall of discharge, allowing temporary storage in ice-marginal channels and braidplains, display a diurnal SSC trend. Linnèlva operates in a dominantly supply limited mode due to the lack of active glacial erosion, with signs of complete sediment depletion over the meltseason. Sedimentation rates are likely to rise as the active layer deepens around the proglacial meltwater stream due to rising temperatures, and proposed increases in the Arctic's precipitation budget allow for high discharge events.

A net mass balance of  $-1.14\text{m}$  water equivalent was measured for Linnèbreen in 2006, producing a volumetric melt of  $.0028\text{km}^3$ . 93.6% of Linnèbreen's mass now lies entirely below the modern ELA at 458m. Extensive mass loss, associated with the ice margin retreat of ca. 1200m from its maximum extent during the LIA, could signal a significant change in thermal regime from its previous inferred warm based structure. The vast

supraglacial and ice marginal meltwater network strongly supports the instrumental data and conclusion that Linnèbreen is composed almost entirely of cold based ice.

The 4-6°C warming at the end of this century proposed by Alley et al (2006), based on the literature and IPCC (2007), is expected to have vast consequences on Svalbard. These temperatures are over two times higher than values estimated for the warmer early Holocene by Hald et al. 2004 and Overpeck et al. 1997. The average ELA on the archipelago was calculated at ca. 450m by Hagen et al. (2003) coinciding with the altitude containing the most ice mass. Further warming, changes in moisture advection, and a freshening of the Arctic Ocean are expected to cause a rise in the regional ELA. This will result in accelerated deglaciation of Svalbard, a situation unprecedented during the Holocene.

## TABLE OF CONTENTS

TITLE PAGE	1
ABSTRACT	2
TABLE OF CONTENTS	4
LIST OF ILLUSTRATIONS	5
1) INTRODUCTION	7
2) BACKGROUND	
2.1 CLIMATOLOGY AND GEOLOGY OF SVALBARD	10
2.2 SVALBARD GLACIERS	13
2.3 HOLOCENE VARIATIONS IN LINNÈDALEN	18
3) METHODOLOGY	
3.1 INSTRUMENT SETUP / FIELD WORK	23
3.2 DISCHARGE / STAGE	26
3.3 SUSPENDED SEDIMENT CONCENTRATION	26
3.4 ABLATION STAKES	28
3.5 AUTOMATED SURFACE LOWERING	28
3.6 MASS BALANCE	29
4) RESULTS	
4.1 ABLATION MEASUREMENTS	30
4.2 YEARLY MASS BALANCE DATA	34
4.3 SUSPENDED SEDIMENT CONCENTRATIONS AND DISCHARGE	35
5) DISCUSSION	
5.1 EXAMINING THERMAL REGIMES	43
5.2 ABLATION DYNAMICS AND SEDIMENT FLUX, A MODERN PERSPECTIVE	46
5.3 SEDIMENT AVAILABILITY	54
5.4 THERMAL REGIME CHANGE AT LINNÈBREEN AND ITS IMPLICATIONS FOR SVALBARD	61
6) CONCLUSIONS	63
7) FURTHER RESEARCH	64
ACKNOWLEDGEMENTS	65
REFERENCES	66

## LIST OF ILLUSTRATIONS

- Figure 1: Observed SAT changes during summer and winter months (ACIS 2004)*
- Figure 2: Location of Svalbard in the Atlantic Region of the Arctic (Przybylak, 2003)*
- Figure 3: Mean annual climatic data recorded at Isfjord Radio, Svalbard (Serreze and Barry 2005)*
- Figure 4: precipitation gradient as you more away from the coast (Humlum 2002)*
- Figure 5: Position relative to warm Atlantic waters advected by the WSC (Hald et al. 2004)*
- Figure 6: ELA map of Svalbard (Hagen et al. 2003)*
- Figure 7: ELA and ice mass distribution (Hagen et al. 2003)*
- Figure 8: SST recustrctions from foram data, IRD flux, and insolation (Hald. et al 2004)*
- Figure 9: Location of Linnèdalen at the outer reaches of Isfjord (Svendsen and Mangerud 1997)*
- Figure 10: Sedimentation rate and characteristics interpreted from lake cores(Svendsen and Mangerud 1997)*
- Figure 11: Bedrock geology of Linnèdalen (Svendsen and Mangerud 1997)*
- Figure 12: Linnèbreen in 1936 at its LIA max*
- Figure 13: Main weather station, glacier up valley in the distance*
- Figure 14: Setup for Campbell SR-50 Snow Sensor at Stake 2*
- Figure 15: Aerial photo of Linnèbreen with instruments / study areas (adapted from Gercke 2006)*
- Figure 16: Vacuum filtration lab showing bottles from ISCO water sampler*
- Figure 17: Grab sample being taken at the toe of the glacier*
- Figure 18: Manual ablation readings, HOBO precip gauge also pictured*
- Figure 19: Cumulative graph of manual ablation stake readings*
- Figure 20: Raw output from Campbell SR-50 snow sensor*
- Figure 21: Precipitation comparison between the glacier and main weather station downvalley*
- Figure 22: Compilation of daily weather and surface lowering recorded at Stake 2*
- Figure 23: Mass Balance and area per altitude distribution on Linnèbreen (Jack Kohler – email)*
- Figure 24: SSC graph comparing upper and lower ISCO sites*
- Figure 25: SSC, discharge, and precipitation correlations at the upper ISCO site*
- Figure 26: Diurnal discharge generally driven by temperature variations*
- Figure 27: Cumulative sediment load computed from upper ISCO site*
- Figure 28: Hysteresis plots for the 2006 field season*
- Figure 29: Grab sample analysis from Linnebreen*
- Figure 30: Vast supraglacial plumbing network on Linnèbreen, black lines designate supraglacial flow, red lines designate ice marginal channels. Grab sample sites are noted by name and color*
- Figure 31: GPS recorded terminal extents and calculated retreat rate on Linnèbreen (Schiff 2004)*
- Figure 32: Linnèbreen during the 2006 field season*

*Figure 33: Summer and Net mass balances on similar Svalbard glaciers (Jack Kohler – email)*

*Figure 34: Popcorn surface texture, carpenters rule for scale*

*Figure 35: Close up of popcorn surface texture*

*Figure 36: Large supraglacial stream which drains from the pool by stake 7*

*Figure 37: Supraglacial pool at stake 7*

*Figure 38: Ice-marginal channel on Linnébreen's left lateral margin*

*Figure 39: Graphical representation of precipitation induced surface lowering*

*Figure 40: SSC comparison from 2006 and 2005 upper ISCO data*

*Figure 41: Precipitation comparison from the three field seasons*

*Figure 42: Weather record for the days leading up to the 7/29 sediment transfer event*

*Figure 43: 2004 modeled SSC and discharge (Matell 2005)*

*Figure 44: 30 year annual summer temperature comparison at Isfjord Radio*

*Table 1: Sedimentation rates related to glacial activity(modified from Matell 2005)*

## 1) INTRODUCTION

Modern process studies, conducted on Arctic glaciers, provide valuable insight into dynamic responses observed in the high latitudes due to global scale climate change, with telltale implications for environmental change in the lower latitudes. Paleoclimatic records, derived from the circum-arctic, suggest a  $1.5^{\circ}\text{C}$  averaged warming over the Arctic during the 19<sup>th</sup> to 20<sup>th</sup> centuries (Overpeck et al. 1997). This area, unfortunately, does not provide us with a long or spatially diverse instrumental record of change. The longest instrumental records available show the Arctic warmed ca.  $0.6^{\circ}\text{C}$  since the beginning of the 20<sup>th</sup> century, an average greater than the northern hemisphere as a whole (Overpeck et al. 1997). Recent climate models, outlined by Alley et al. (2006), predict annual temperatures in the Arctic continue to will warm by  $4\text{--}6^{\circ}\text{C}$  by the end of the 21<sup>st</sup> century.

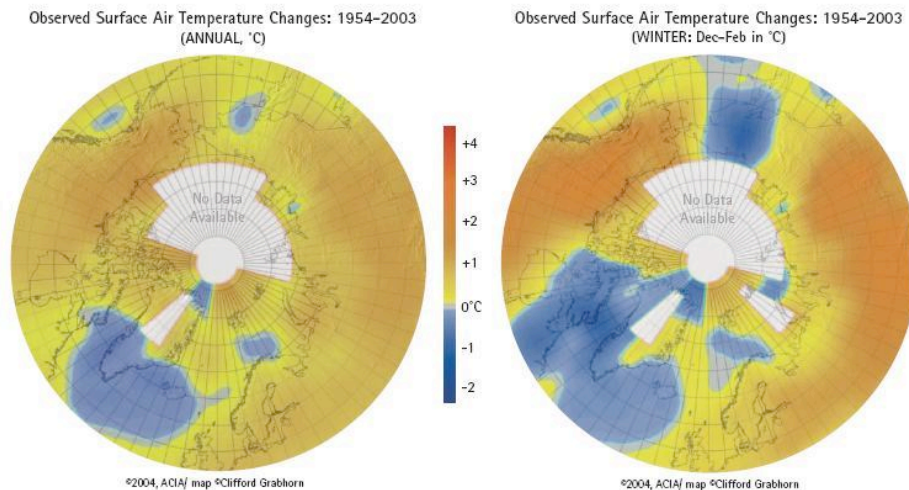


*Figure 1: Observed SAT changes during summer and winter months (ACIS 2004)*

Warming is amplified in the Arctic due to a number of positive feedback cycles. Net radiation inputs are greater at the equatorial regions of the Earth as the sun's rays hit at a more direct angle. This uneven distribution results in both a pressure gradient in the

atmosphere and density gradient in the ocean, driving circulation of the whole Earth system. As such, the Arctic effectively acts as a heat sink to the equatorial region and provides an energy balance over the planet (ACIS 2004). Anthropogenic greenhouse gas (GHG) loading of the atmosphere and ecosystem destruction on land are pushing our globe into a state well beyond the scope of natural variability (IPCC 2007). The long term Pleistocene “Ice Ages” were driven by Milankovitch orbital variations, during this time, processes acted within the various components of the Earth system to keep atmospheric CO<sub>2</sub> within 180-280 ppm and CH<sub>4</sub> within 250-770 ppb during the glacial-interglacial cycles respectively. Current concentration values, 379 ppm CO<sub>2</sub> / 1774 ppb CH<sub>4</sub>, are anticipated to increase without bound as population grows and ecosystems are destroyed (IPCC 2007). These factors provide renewed momentum into understanding the role of the Arctic within the global climate system.

The broad goal of the NSF Svalbard REU program, now in its third year, is both to expose undergraduate students to the Arctic research environment, and to better understand the influence of modern processes on sedimentation patterns in the glacial/fluvial/lacustrine environments of Linnèdalen. This study allows for better interpretation of the historical data recorded in lake sediments and production of a high-resolution record of regional climate change for comparison with other Arctic regions. The objective of this study is to expand upon previous studies of Linnèbreen and to interpret the high resolution ablation/ suspended sediment concentration (SSC) data taken during the summer of 2006. By comparing high resolution meteorological, glacier ablation, and suspended sediment data the main agent of surface lowering and mass loss on Linnèbreen is determined. These interpretations allow us to understand the suspended

sediment concentrations in pro-glacial stream Linnèelva and ultimately sediment deposition rates in Linnèvatnet. Svalbard's position relative to atmospheric and oceanic circulations creates a sensitive environment as contrasting air masses create dramatically varying weather. It is important to characterize and understand the signals in Svalbard's glacial landscape as regional climate pushes into new territory.

This thesis provides a historic overview of Svalbard's varying climate, allowing a basis for this current study under the concept of the past being the key to the future. This is followed by a description of our methodology while collecting data in the field and analysis in the lab. Data recorded from the network of instruments on and around the glacier is presented and discussed in respect to deviations in surface lowering and sediment flux. This allows the correlation of meteorological forces to both physical changes on Linnèbreen and the supply of sediment transported down valley. I will conclude with a discussion of the results, providing a comparison to previous data, the mass balance of Linnèbreen, and Svalbard's glacial landscape. Results from this study are applied to the entire archipelago and compared to similar high Arctic locations in respect to the warming climatic state of the Arctic.

## 2) BACKGROUND

### 2.1 Climatology and Geology of Svalbard

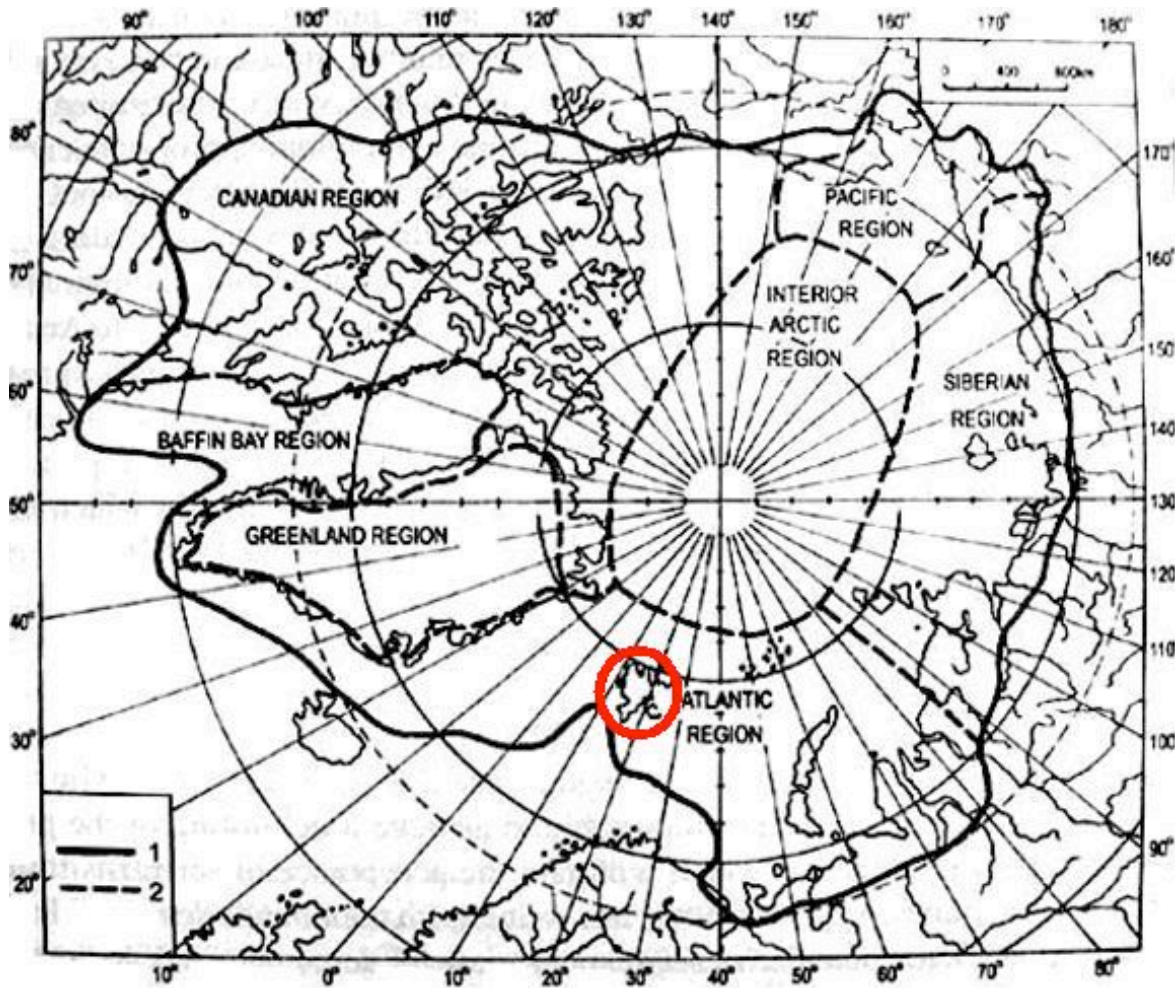


Figure 2: Location of Svalbard in the Atlantic Region of the Arctic (Przybylak, 2003)

The Arctic climate system is a dynamic environment, closely coupled with interactions between the ocean, atmosphere, and land. Svalbard, a 62,000 km<sup>2</sup> archipelago (76° to 80° N), is located north of Norway in the high-Arctic and bordered by the Arctic Ocean to the North, the Barents Sea to the South/East, and the Norwegian-Greenland Sea to the West. Svalbard is composed of mostly Phanerozoic sedimentary rock and currently covered by 2100 ice masses, equaling about 37,000 km<sup>2</sup> of area, ~60% of the total area in Svalbard (Hodgkins 1997). The total volume of ice is estimated to be

7000km<sup>3</sup>, approximately 0.02m of sea-level equivalent (Hagen et al. 2003). Several of these ice masses are tide-water glaciers, calving into the ocean or the numerous fjords that cut into the landmass.

The Atlantic sector of the Arctic, containing Svalbard, is characterized by a maritime Arctic climate, full of clouds, high humidity, narrow annual temperature range, and typically high precipitation rates (Serreze et al. 2005). Oceanic and atmospheric circulation bring sensible and latent heat to the Arctic in order to make up for the atmospheric radiation imbalance at high latitudes. Even though Svalbard is in 24-hour sunlight during the summer months, it is still well below the global average of 340Wm<sup>-2</sup>.

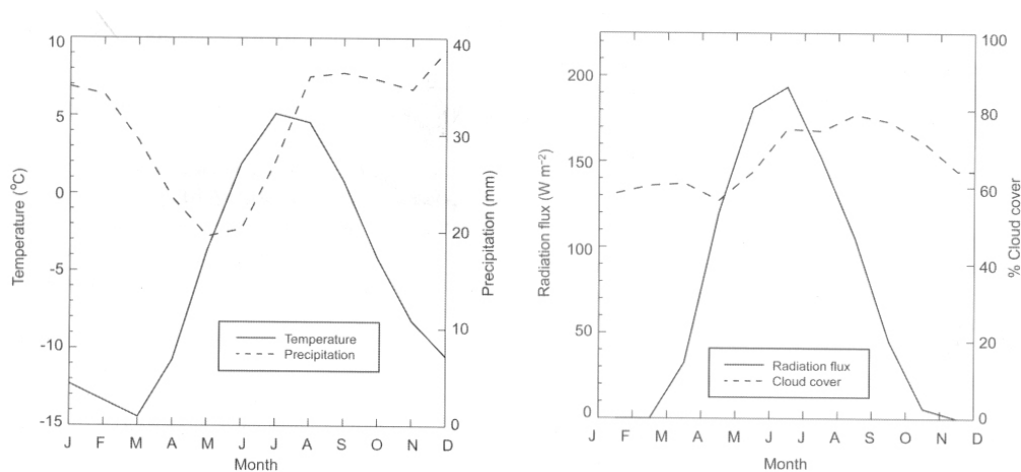


Figure 3: Mean annual climatic data recorded at Isford Radio, Svalbard (Serreze and Barry 2005)

Pressure gradients are created by the Icelandic low and induced flow over the Greenland Ice Sheet and Arctic Ocean. This drives warm moist air from the North Atlantic where it contrasts with the easterly High Arctic polar air mass, creating dramatically varying weather. This gradient and weather variability intensifies in the winter months as sea ice amplifies the contrast between air masses.

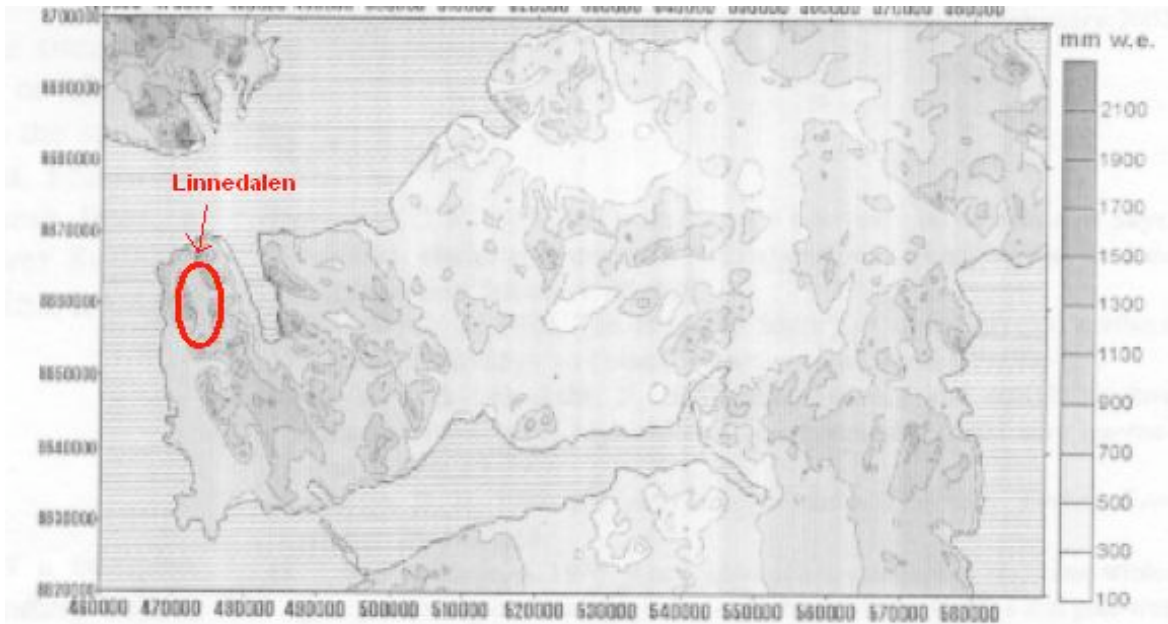
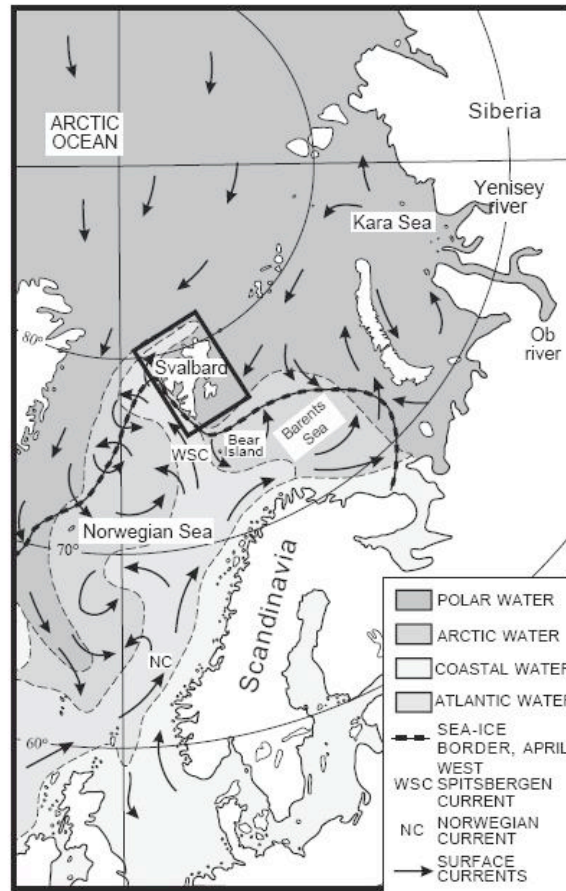


Figure 4: precipitation gradient as you move away from the coast (modified from Humlum 2002)

High precipitation, characteristic of this section of the Arctic, is not the case everywhere on Svalbard. Moisture advection and orographic effects cause the central portion of Spitsbergen to be a polar desert, ~190mm w.e. measured in Longyearbyen. This directly contrasts with the record at Isfjord Radio on the west coast of Spitsbergen, close to the study area. Here the record of annual precipitation averages 430mm w.e. This dissimilarity reflects a significant precipitation gradient as one moves from the coast across the mountains into central Spitsbergen. Glaciers in this region survive by accumulation of wind blown snow on their surfaces, and many valley glaciers, located in-between plateaus, receive snow which is easily carried horizontally and deposited in the valley.

Svalbard's proximal position to the northern influence of the Gulf Stream allows a warmer and moister climate than adjacent NE Greenland. Warm Atlantic waters are carried up along the western coast of Spitsbergen by the West Spitsbergen Current, providing the islands with a mean annual temperature of -6°C. For six months of the

year, Svalbard is surrounded by pack ice, though its thickness dwindles along the western margin because of warm ocean currents (Hald et al. 2004).



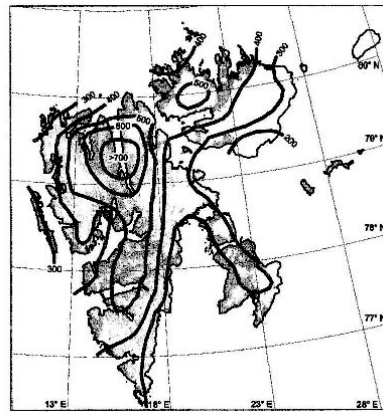
(A)

Figure 5: Position relative to warm Atlantic waters advected by the WSC (Hald et al. 2004)

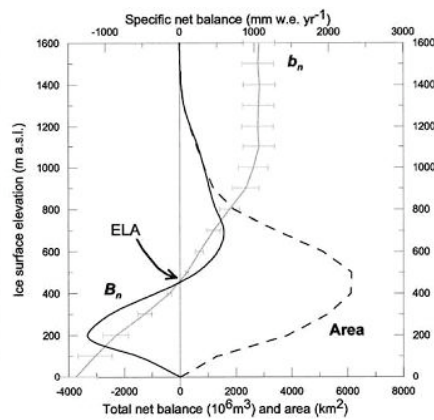
## 2.2 Svalbard Glaciers

Svalbard’s glaciers, generally flat and uncrevassed, are sensitive to its varying climate and Gulf Stream influence. Glaciers in the Arctic experience higher temperatures than those in the Antarctic, and therefore have a quicker response to the changing climate (Hagen et al. 2003). Svalbard’s abundant ice masses provide an important and accessible area to examine glacial dynamics. Hagen et al (2003) described the overall net mass balance of ice masses in the archipelago. This was a difficult task to accomplish

because field measurements have only been taken over 0.5% of the glaciers, and mainly on small cirque glaciers at low elevation (Hagen et al. 2003). Svalbard was divided into 13 regions based on major drainage basins, and a net mass balance per altitude curve was estimated based on field measurements, point net balance measurements from reference horizons in shallow ice cores, snow distribution maps from ground penetrating radar, and ELA distribution maps from aerial and satellite images (Hagen et al. 2003). The resulting ELA map greatly resembles the precipitation pattern with coastal areas receiving more precipitation, greater accumulation, resulting in lower ELA's. The overall net surface mass balance for the combined 13 regions was estimated to be  $-0.5 \pm 0.1 \text{ km}^3 \text{ yr}^{-1}$  with a mean specific surface net mass balance is  $-14 \text{ mm} \pm 3 \text{ mm yr}^{-1}$  of melt water equivalent (Hagen et al. 2003).



6



7

Figure 6: ELA map of Svalbard (Hagen et al. 2003)  
 Figure 7: ELA and ice mass distribution (Hagen et al. 2003)

Svalbard also contains an array of tidewater glaciers that collectively represent  $\sim 1000 \text{ km}$  of calving margin. Though this ice is slow moving, the total estimate for calving ice flux and retreat of ice fronts is around  $4 \pm 1 \text{ km}^3 \text{ yr}^{-1}$  (Hagen et al. 2003). This combined with the surface mass balance to give us a rough estimate to the total net

balance of Svalbard,  $-4.5^{+/-} 1 \text{ km}^3 \text{ yr}^{-1}$  with a specific balance of  $-120^{+/-} 30 \text{ mm yr}^{-1}$  of melt water equivalent (Hagen et al. 2003). Through area/altitude distribution analysis, an average ELA of ca. 450m was determined for Svalbard, equivalent to the altitude containing the greatest area of ice mass (Hagen et al. 2003). Svalbard's glacial cover is extremely sensitive to changes in climate due to its abundance at the modern ELA. Further warming and resultant rise of the regional ELA will greatly reduce the volume of ice on Svalbard.

Svalbard's high latitude, low mass-balance gradient, glacial environment is in direct contrast to the characteristic temperate thermal regime and high mass balance gradient found in subpolar-tropical regions (Hodgkins 1997). This gradient represents the change in mass balance per change in altitude. Temperate glaciers, composed of warm based ice, are at the pressure melting point through the glacial ice, providing an englacial and subglacial network for meltwater to permeate and flow. Warm based ice can form on Svalbard through deep ice at the pressure melting point or by meltwater percolating into the snowpack and refreezing ("firn-soaking"), releasing latent heat into the ice (Hodgkins 1997). Once the basal layer begins to slide the frictional heat generated further promotes this condition. Cold based ice generally restricts meltwater penetration, leaving it contained and transported rapidly on the surface and in ice marginal channels. These glaciers display relatively low glacier activity because they are frozen to their bed, crevasses are uncommon. Movement is attributed to the slow deformation of ice, maintaining the structure of underlying bedrock.

Glaciers of Svalbard can range from cold-based to polythermal glaciers. Hodgkins (1997) examined three ice masses from Spitsbergen, Scott Turnerbreen

(entirely cold based), Austre Broggerbreen (cold based, except for a layer near its bed), and Kongsvegen (polythermal). During the meltseason, meltwater saturates the snowpack, refreezes at the glacier surface releasing latent heat, and starts runoff down the glacier (Repp 1988). The solid layer created on the glaciers surface contains meltwater transportation on the surface. This contributes to the formation of supraglacial lakes and slush areas in glacial depressions, noted to form in late May-June and last up to 2 months (Liestol et al. 1980, Hagen et al. 1991, Vatne et al. 1996). Hagen (1991) observed these lakes reaching their maximum size in 2 weeks but draining in only 1-2 days when a supraglacial channel opened. Average glacier runoff rises in June, is strongest in July and August, and tapers dramatically by September. Peak discharges were recorded early in the melt season, after which they only occurred when maritime weather systems moved through the area (Hodgkins 1997). This illustrates the importance of the West Spitsbergen Current in advecting moisture over Svalbard and contributing to dynamic behavior of the glaciers and regional climate.

Hodgkins (1997) examined meltwater fluctuations on Scott Turnerbreen, a cold based glacier, and found that high discharge early in the melt season was attributed to net losses from supraglacial storage on the glacier. In the latter portion of the melt season there was much less discharge, though it showed a diurnal signal and was linked to air temperature and solar radiation values (Hodgkins 1997). This shows two distinct modes of discharge that are modulated by meltwater storage on the glacier. After these reservoirs are emptied, the glacier shows greater response to meteorological forcing because the meltwater signal is not muted by the addition of stored meltwater (Hodgkins 1997).

Suspended sediment, carried down glacier through the pro-glacial environment, has close ties to glacier basal thermal regime, discharge rates, and thus regional meteorological forcing. Through the entire meltseason, there is a general rise in suspended sediment concentrations (SSC) on Svalbard, contrary to the early season flux on temperate glaciers determined by Bogen (1991). This could have implications for the liberation of more sediment during summer warming and thawing; adding to the available supply for meltwater erosion. Different studies attribute high SSC in temperate glaciers to early meltseason erosion of sediment stored during the winter season (Hodgkins 1997). Hodson's (1994) study of proglacial and sandur plain outlet areas in front of Austre Broggerbreen established that most of the transported sediment is contributed by the glacial environment instead of sediment entrained in the meltwater stream and its tributaries. It was originally thought that active layer thawing would add significant spikes to the SSC in the meltwater channels on the plain; however, it occurred simultaneously in both. Permafrost processes may influence sediment availability over time around Svalbard's glaciers, moving their sources further up the lateral sides of glaciers during the meltseason (Hodgkins 1997).

A five year study by Repp (1988) determined that diurnal SSC peaks came two hours before peak discharge rates. As the meltseason continues, this lead time becomes more and more diminished. This can be attributed to storage in ice marginal channels along non-temperate glaciers. As discharge falls late in the season, sediment is stored in pools in the marginal channels only to be re-mobilized during higher discharge event suchs caused by snowmelt or precipitation (Hodgkins 1997). This differs from temperate

glaciers whose channels will close during low discharge because of high ice deformation rates (Hodgkins 1997).

### 2.3 Holocene Variations in Linnèdalen

The abundance of temperature sensitive planktonic foraminifera in marine cores produces a good proxy for local sea surface temperature (SST). Hald et al. (2004) combined foram data and IRD flux from Van Mijenfjord, the second largest fjord on Spitsbergen, to show a warm early, cooling middle, and generally stable and cool late Holocene.

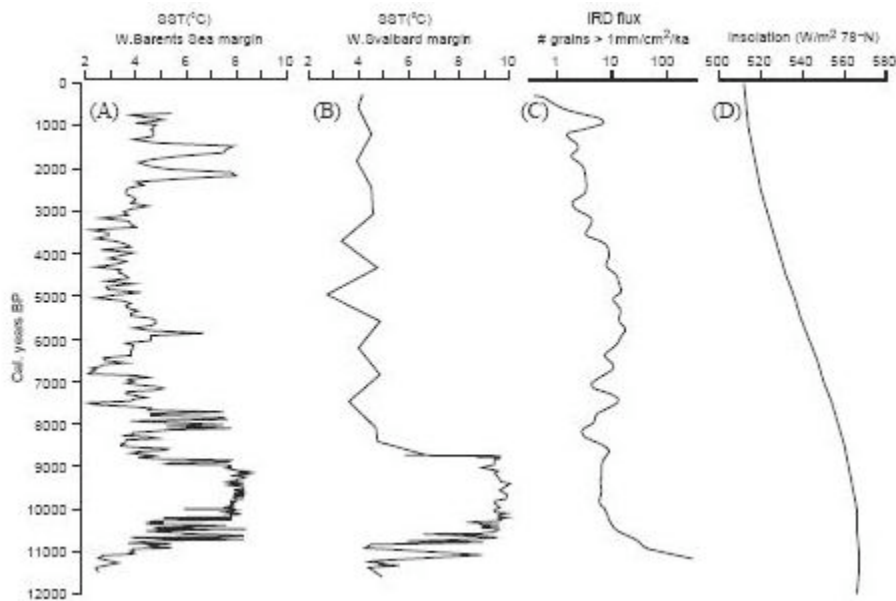


Figure 8: SST reconstructions from foram data, IRD flux, and insolation (Hald. et al 2004)

This is strikingly similar to the Mangerud et al. (1998) trends based on orbital forcing and peak insolation at the northern latitudes (figure 8). The seemingly abrupt change in the proxy record is due to low sedimentation rates relative to the early Holocene and associated sediment exhaustion and glacio-eustatic fall / erosion (Hald et al. 2004). The presence of IRD in the continuous cores tells us that central Spitsbergen was never completely deglaciated during the Holocene (Hald et al. 2004).

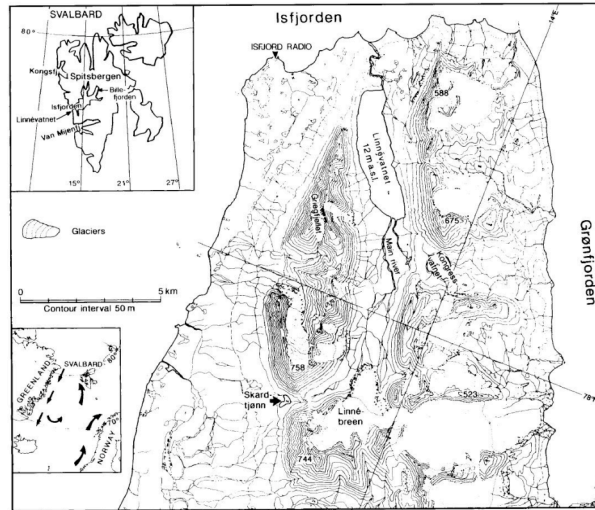


Figure 9: Location of Linnédalen at the outer reaches of Isfjord (Svendsen and Mangerud 1997)

Linnédalen is located at the mouth of Isfjord facing the Arctic Ocean on the western edge of Spitsbergen. Linnèvatnet is a 4.7km long, 1.3km wide lake that contains sediments from both late glacial marine and Holocene lacustrine environments. Bulk radiocarbon dating of lake bottom sediments proved to be a problem in past studies (Boyum and Keijensmo 1978), resulting from the coal bearing sandstone bedrock with lies in the center of the valley and underneath Linnébreen (Snyder et al. 1993). Denudation rate comparisons from glaciated and non-glaciated areas suggest that glacial erosion is more efficient than any other erosional process on Svalbard (Svendsen et al. 1989). The sliding nature of this inferred temperate glacier likely caused heavy erosion of its underlying surface; thus a supply of coal to Linnèvatnet. Coal additions, which are  $^{14}\text{C}$  dead, into the organic content of the lake sediments effectively contaminates ages derived from the bulk sediment (Snyder et al. 1993). This adds to the already low non-coal organic content in the lake. Bulk dating shows age offsets of over 10,000 years (Snyder et al. 1993). Snyder et al (1993) were able to use terrestrial plant microfossils from inlet proximal cores to date accurately and correlate to the more distal records in the center of the lake.

Striations, found on the bedrock along the lateral sides of Linnødalen, point to northerly flow of ice during the Late Weichselian max. Svendsen and Mangerud's (1997) analysis of lake cores tells us that after deglaciation, marine mud from the lake bottom shows Linnødalen was a tributary fjord of Isfjord. Resultant isostatic uplift subsequent to deglaciation effectively cut Linnøvatnet off from the ocean around 9600 yr B.P. (Svendsen and Mangerud 1997). Early Holocene lake sediments are massive in texture and contain high amounts of CaCO<sub>3</sub>, derived from limestone on the eastern side of the valley (Svendsen and Mangerud 1997).

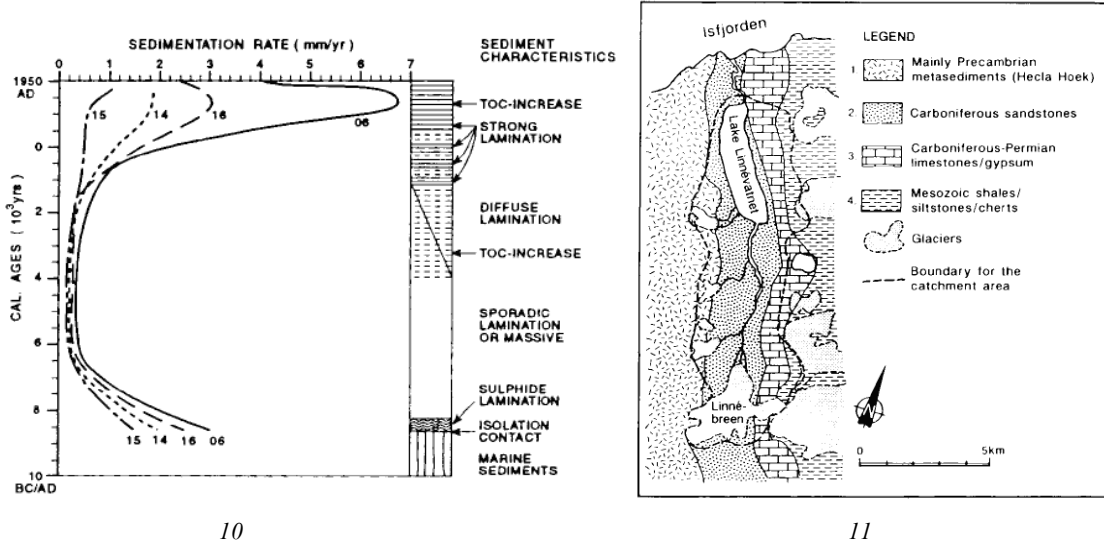


Figure 10: Sedimentation rate and characteristics interpreted from lake cores (Svendsen and Mangerud 1997)  
 Figure 11: Bedrock geology of Linnødalen (Svendsen and Mangerud 1997)

Their interpretation of the early Holocene suggests there was no glacier present in Linnødalen during this time (Svendsen and Mangerud 1997). This notion is consistent with the high obliquity values for this time interval as pointed out by Mangerud et al. (1998). The warm early Holocene, predicted by forams, corresponds in Linnødalen to the disappearance of the valley glacier, implying temperatures 1.5-2.5°C higher than present (Hald et al 2004). Plant macrofossils described by Birks (1991) on the outer banks of Isfjord and work by Overpeck et al. (1997) agree with temperatures being ~2°C warmer.

Increases in coal content and laminations in lacustrine sediment around 4400 yr B.P. implies the formation of Linnèbreen up valley (Svendsen and Mangerud 1997). The coal bearing sandstone, which resides beneath Linnèbreen, is easily eroded making coal content a proxy for glacial activity as outlined earlier. Peak sedimentation, distinct laminations, and high coal concentrations all occur in Linnèvatnet during the Little Ice Age (LIA), representing the Holocene maximum extent of Linnèbreen and numerous other Svalbard glaciers.



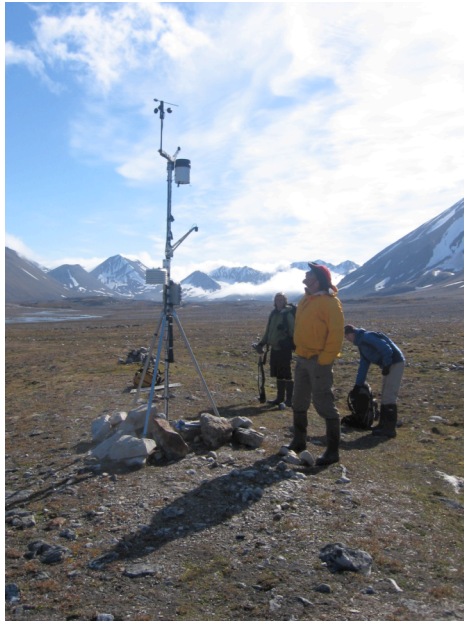
*Figure 12: Linnèbreen in 1936 at its LIA max*

The cause for the LIA is highly debated, however, a 40% increase in volcanism and low solar output interpreted from low sunspot concentrations are attributed to its culmination (Serreze and Barry 2005). The large LIA ice cored moraine stands as a prominent feature today in front of Linnèbreen, which also allows us to calculate its current retreat. This is

also documented by Svendsen and Mangerud (1997) using decreased coal concentration and sedimentation rate in Linnèvatnet. After 1920, there was a rise in mean annual air temperature of ca 5°C, linked to the termination of the LIA (Hodgkins 1997). Svalbard's ice masses are currently reacting with net losses in order to maintain equilibrium with this changing climate.

### 3) METHODOLOGY

#### 3.1 Instrument setup / Field Work



13

Figure 13: Main weather station, glacier up valley in the distance



14

Figure 14: Setup for Campbell SR-50 Snow Sensor at Stake 2

During our field season, from July 18<sup>th</sup>- August 15<sup>th</sup>, a compilation of mass balance measurements, local meteorological data, stream gauge, and suspended sediment concentrations were recorded in Linnédalen. A number of high resolution instruments were set up in order to correlate signals in the glacier, stream, and lake systems to external factors. An automated HOBO weather station, located near the south end of Linnèvatnet, was used to record an array of meteorological data, including; air temperature, 0.5 and 1m soil temperature, wind speed/direction, precipitation, relative humidity, barometric pressure, and upward/downward solar radiation at 30 minute intervals. These instruments supplied a high-fidelity local record of overall weather in Linnédalen.

In order to better document conditions on the glacier, located 8km up valley, six monitoring instruments were deployed on or adjacent to the glacier. These included three HOBO air temperature loggers, set up on the LIA moraine, 195 m, and 340m asl along the left lateral. In order to capture high resolution surface lowering data, we installed a Campbell SR-50 snow sensor on the glacier. A 3 meter galvanized aluminum pole was drilled into the glacier, at 195m next to ablation stake 2, in order to mount this instrument perpendicular to the glacier's surface. A solar panel and charge regulator were also installed in order to conserve battery use in the 24 hour summer sun. Two HOBO radiation sensors were zip tied to the mounting, one facing up to measure incoming radiation from the sun, and the other facing down to measure outgoing radiation off the glacier. A HOBO Onset RG3-M tipping bucket rain gauge was installed on ablation stake two, five meters from the snow sensor, to directly measure rainfall. The 30-minute sampling interval on these instruments gave high resolution readings exclusive to Linnébreen's surroundings, allowing for comparisons between surface lowering and concurrent meteorological fluctuations. Like the weather station, each of these instruments was programmed to document changes at 30 minute intervals. To quantify the sediment flux of the proglacial stream Linnèlva, ISCO automatic water samplers were setup in proximal (1.2km) and distal (8km) locations to the glacier. An intake tube was positioned in the stream's center, 40cm above the stream bed, and attached to a steel stake with cable ties. These instruments were programmed to siphon 450mL of water every two hours. To speed up filtering time, samples were eventually decreased to 250mL a week into the field season.



Figure 15: Aerial photo of Linnëbreen with instruments / study areas (adapted from Gercke 2006)

### *3.2 Discharge / Stage*

Discharge readings were taken in 1 meter increments with a meter stick and Swoffer current meter from the prominent mud flat area by the prominent LIA moraine in front of Linnèbreen. Carr (2006) calculated discharge by multiplying the average channel velocity by the cross sectional area. River stage was determined every five minutes using a Solinst level logger. This instrument, attached to a steel stake, measured the pressure of the overlying water column. Level logger stage readings were corrected for barometric pressure by subtracting the weather station barometric readings after they were converted to cm water. This was calculated by multiplying the barometric reading, in mb, by 1.0198. Svalbard REU Co-director, Steve Roof, produced a stage/discharge rating curve by using average stage values during discharge reading times. Trendlines were added by linear and exponential equations. A continuous discharge record was then produced by using the trendline equations to convert stage to discharge.

### *3.3 Suspended Sediment Concentration*

Grab samples were taken from the discharge monitoring site and from one .8km in front of the glacier at around 1245 (figure 15). Two additional meltwater samples were taken from a large supraglacial stream near the cirque, (@ 1445) and a large ice marginal stream by the toe of the glacier (@ 1515). These grab samples, 250ml in volume, were contained in 1 liter Nalgene bottles from the center of the stream half way into the water column every other day. The purpose of these samples was to document areas in the glaciers environment that act as sediment batteries/sinks.



*Figure 16: Vacuum filtration lab showing bottles from ISCO water sampler*

The sediment filtering lab, installed at Isfjord Radio, was used to determine the total suspended sediment contained in the volume of each ISCO or grab sample. All samples were vacuum filtered through pre-weighed cellulose nitrate Whatman membrane filters, with a 0.45µm pore size. After all of the water was removed by the vacuum, membranes were set aside to air dry for a 24 hour period. The membranes were then weighed and sediment concentrations were determined in mg/L by removing the mass of the filter and dividing by sample volume.  $[(\text{filter} + \text{sediment mass}) - (\text{filter mass})] / (\text{water sample volume})$  (Carr 2006).



*Figure 17: Grab sample being taken at the toe of the glacier  
Figure 18: Manual ablation readings, HOB0 precip gauge also pictured*

### *3.4 Ablation Stakes*

Manual ablation readings were taken from the eight centerline galvanized aluminum poles, installed during the 2004 field season. They were augured into the glacier ~250m apart from each other, covering an altitude from 161-378m asl (figure 15). These poles are 6 meters in length and are replaced as they melt out due to extensive surface lowering. Readings were taken by representing the surface with a plywood board and marking the pole perpendicular to north each glacier day. This process began at 1300 and finished around 1430 near the cirque. Marks were then measured with a meter stick for each two day increment up until the last glacier day, August 12<sup>th</sup>. Readings were taken in similar fashion in 2005 and 2004, though a greater number of lab days produced gaps between readings in 2004.

### *3.5 Automated Surface Lowering*

Automated measurements were taken by the Campbell SR-50 Snow Sensor for the first time this field season. This instrument gave us the temporal ability to document weather and correlate it to behavior in the glacial environment. The snow sensor sends out an array of ultrasonic pulses (50kHz) at an angle of ~22° and recorded echoes. The measured speed of sound is air temperature dependent and required the use of an external air temperature sensor to calculate the corrected distance by use of the equation  $DISTANCE = READING(\sqrt{T^{\circ}KELVIN / 273.15})$ . The instrument took readings every 30 minutes at 0.1mm resolution.

### *3.6 Mass Balance*

Mass balance measurements were taken by Jack Kohler of the Norwegian Polar Institute. Winter balance is calculated from an array of snow depth soundings, stake height, and snow density measurements at the end of the accumulation period in May. (Kohler – unpublished) Summer balance is calculated from comparisons of fall stake measurements to those in May (Kohler – unpublished). Extrapolation from aerial photographs allows balance estimates to extended over the glacier in 50m intervals (Kohler- unpublished)

## 4) RESULTS

### 4.1 Ablation Measurements

From our manual recording period of July 23<sup>rd</sup> – August 12<sup>th</sup>, the amount of surface lowering of the glacier, for each two day period, was compiled and compared up the glacier (figure 19). Surface lowering values ranged from 91.3cm at stake 1a to 58.15cm at stake 5. Even at stake eight, the upper most stake, the surface lowered 60.35cm during this period. Stakes 1a / 7a are the replacements for stakes 1 and 7, installed in 2004, which are currently melting out of the ice. Lowering rates were determined to average 4.8cm of lowering per day at the toe and 3.18cm at the cirque for this 21 day manual reading period.

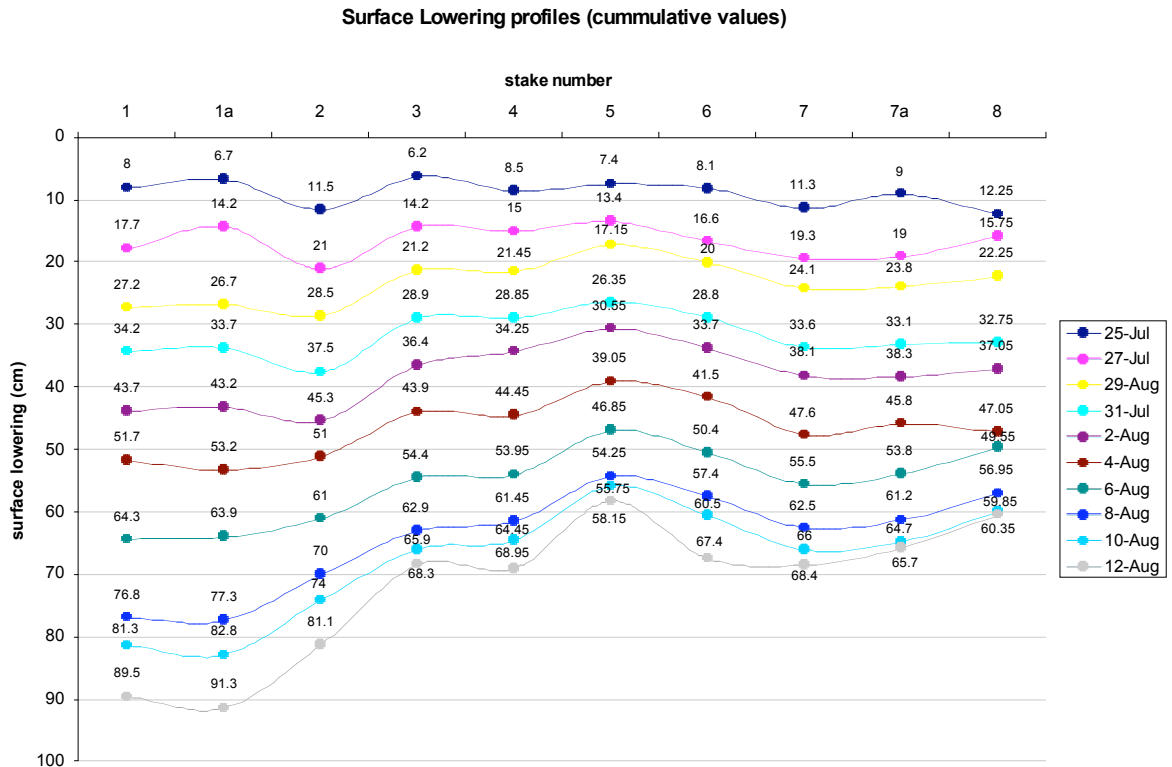


Figure 19: Cumulative graph of manual ablation stake readings

A much higher resolution record was attainable from the Campbell SR-50 snow sensor, setup next to stake two. The raw output from this instrument, with temperature correction, is shown in figure 20.

### Raw Output from Snow Sensor

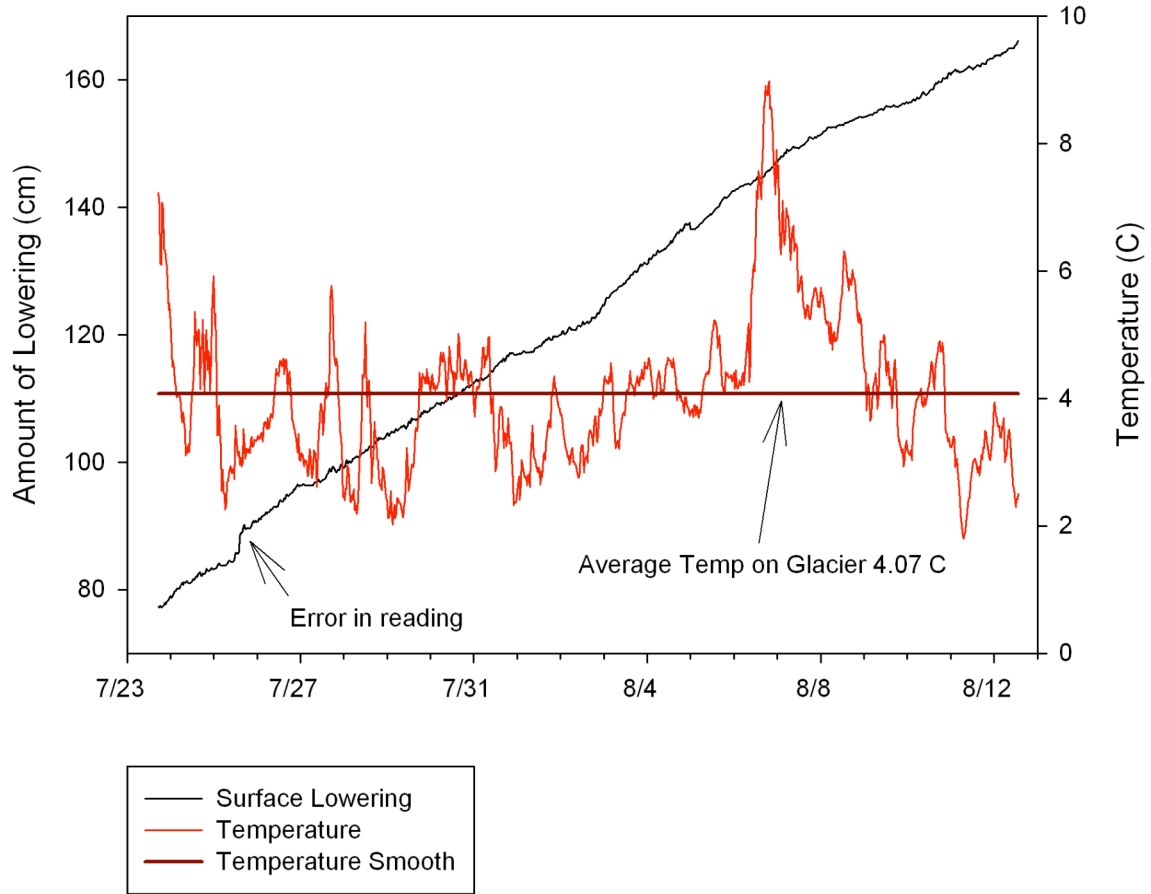


Figure 20: Raw output from Campbell SR-50 snow sensor

From this graph it is clear that the distance between the sensor and the surface of the glacier became greater with time. At the end of July 25<sup>th</sup>, there is an abrupt 3cm jump in surface lowering and is assumed to be an error caused by the movement of the instrument. Two days of lowering data before this error are omitted from analysis. In total, this instrument recorded a lowering of 77.2cm during its adjusted 19 day recording period from July 25<sup>th</sup> 15:00 to August 12<sup>th</sup> 13:30. The graph looks fairly linear overall.

However, there are a few periods of slope change which require further analysis with respect to meteorological forcing.

The average temperature on the glacier during our recorded period was 4.07°C, over a degree colder than the 6.5°C average temperature recorded down valley during the same interval. To examine the meteorological differences between these two areas, 8km apart, precipitation graphs were also compared. Both recorded 12.2mm of precipitation at different times and intensities during this period (figure 21). Without a wind baffle on the precip gauge at Linnèbreen, it seemed that katabatic winds might influence the readings. This was shown, however, not to be case as there were equal totals at both sites.

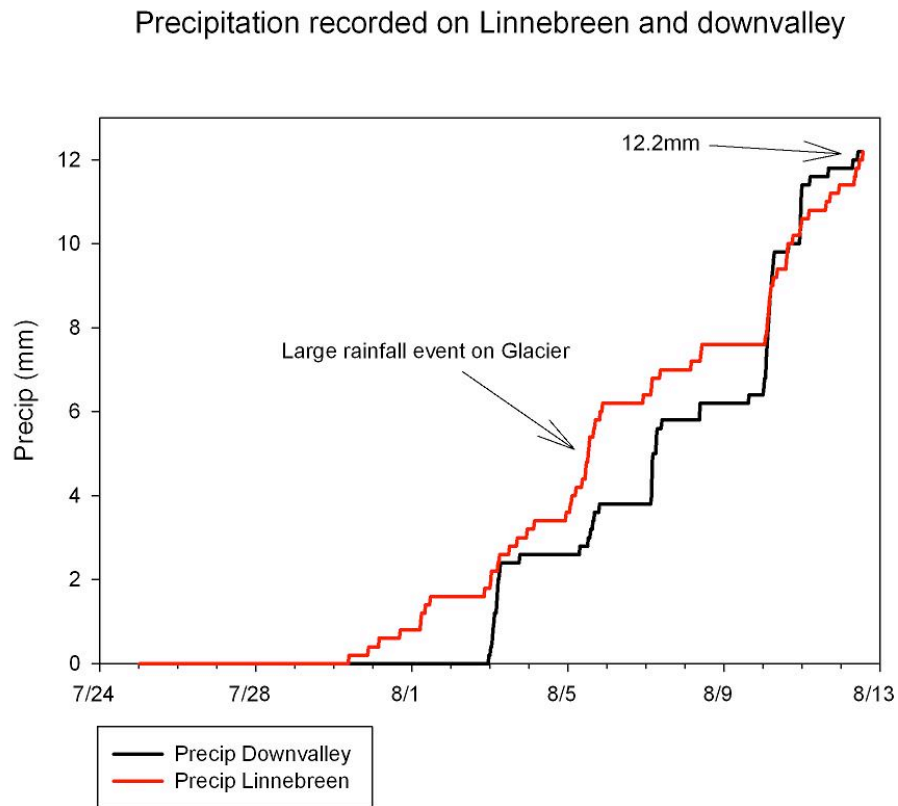


Figure 21: Precipitation comparison between the glacier and main weather station downvalley

From figure 21 we established the importance of monitoring all data within a proximal location to the study. What appeared as a minor rainfall on Aug. 5<sup>th</sup> downvalley, was in fact a significant event on the glacier, a telltale sign of the importance in monitoring microclimates during a spatially widespread modern process study. The precip event on August 5th certainly affected signals in all systems of Linnédalen.

To characterize surface lowering on the glacier, all data recorded at or near ablation stake 2 was compiled graphically with daily values.

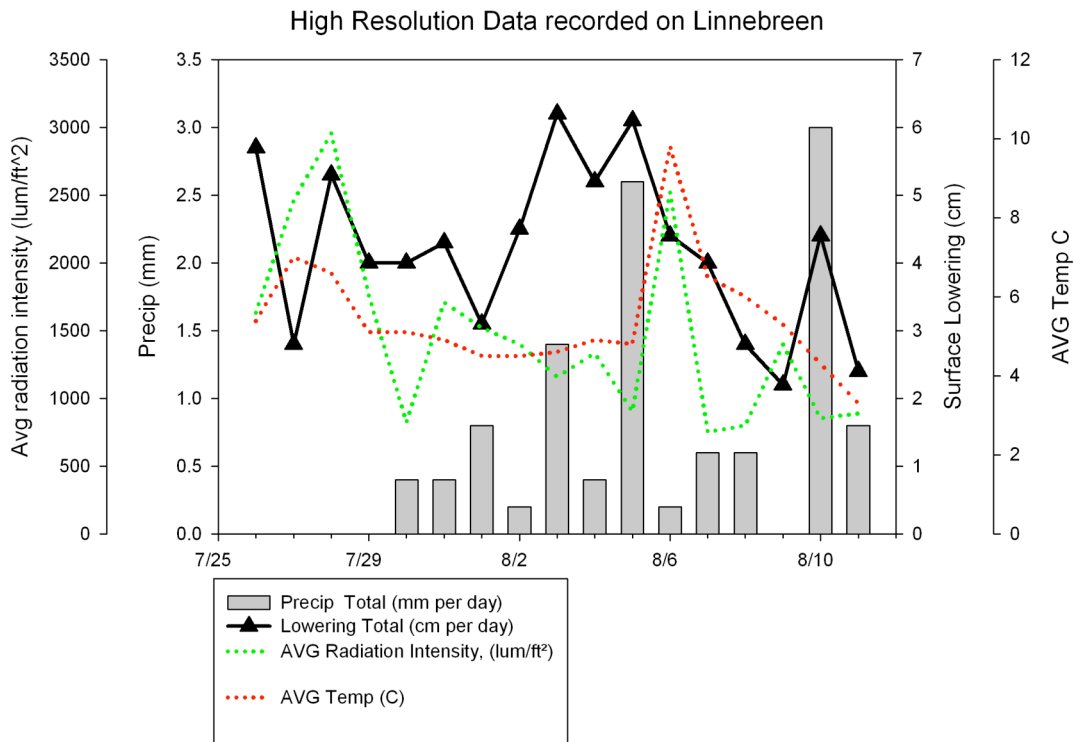


Figure 22: Compilation of daily weather and surface lowering recorded at Stake 2

Major rainfall events line up with peaks in total glacier surface lowering. Though certainly part of the big picture, neither solar radiation or air temperature had such a direct connection to the lowering data. For this reason, I suggest that summer precipitation is the main agent of surface lowering on Linnébreen. This conclusion is

part of the large scale picture of what is occurring to Linnèbreen with respect to the changing climate post LIA.

#### 4.2 Yearly Mass Balance Data

Mass balance data, collected over 2005-2006 by Jack Kohler, Norwegian Polar Institute, shows the summer, winter, and net mass balance on the glacier plotted with altitude/ice area distribution.

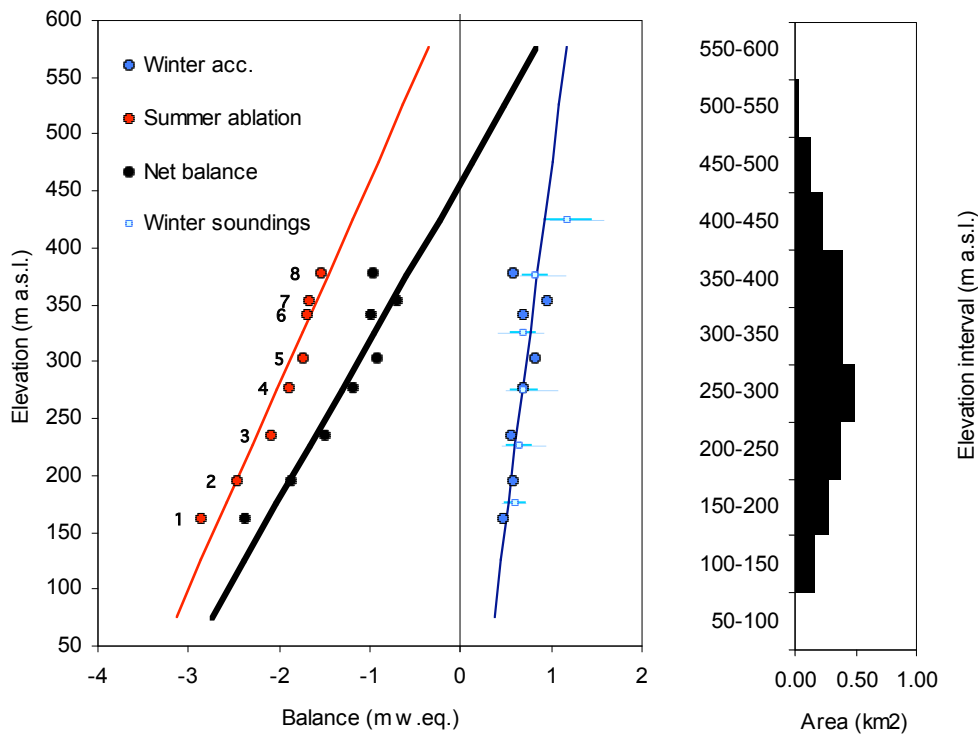


Figure 23: Mass Balance and area per altitude distribution on Linnèbreen (Jack Kohler, pers. comm.)

The net winter accumulation was 0.74 meters of water equivalent (m w.eq.). This ranged from 0.48 at stake 1 by the toe to 0.97 m w.eq. at stake 7. Accumulation generally increased with altitude except for 0.58 at stake 3, 0.69 at stake 6, and 0.58 at stake 8 by the cirque. Net summer ablation totaled -1.88 m w.eq. on Linnèbreen. Ablation was highest at the toe, measuring -2.85 m w.eq. at stake 1, up to -1.53 m w.eq. at stake 8 by the cirque. The net mass balance of the glacier was calculated to be -1.14m w.eq.,

producing a net volumetric melt of  $0.0028\text{km}^3$ . Sample extrapolation allows the net balance per altitude line can be extended above the ablation stakes. This places the modern ELA for Linnèbreen at 458m during the 2006 ablation season, with 93.6% of the glaciers mass entirely below this point.

#### *4.3 Suspended Sediment Concentrations and Discharge*

During the 2006 six field season, suspended sediment concentrations (SSC) recorded at both ISCO water samplers showed staggered diurnal cycles (figure 24). Peaks in upper ISCO SSC came approximately four hours before the lower ISCO SSC. These sites also varied by a factor of 4 in amplitude, the upper ISCO SSC values ranged between 178.9-4474.6 mg/L where as the lower ISCO measured sediment concentrations between 16.7-754.8 mg/L. The difference between the two sites is tied to the storage of larger sediment in the mudflats and braidplain of Linnèelva (Matell 2005). Despite the lag and the difference in SSC, both sites appear to respond in a comparable manner from 7/21/06-8/5/06. From 8/6/06-8/10/06, both sites show a muted signal. There were no high amplitude changes in sediment release until the upper site jumps abruptly on 8/10/06 during the largest rainfall of the season (3.0mm).

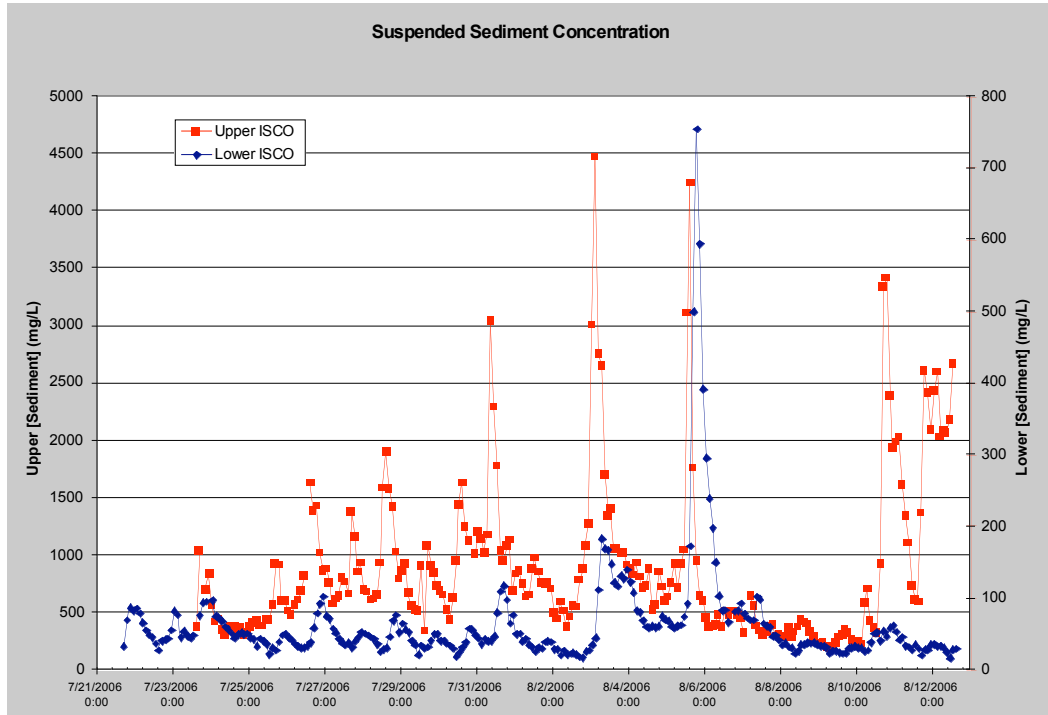


Figure 24: SSC graph comparing upper and lower ISCO sites

Because the upper ISCO site records high resolution stream data proximal to the glacier, further examination to the cause and effect of discharge on SSC in Linnèlva is in respect to this instrument. Higher velocity discharge carries a denser concentration of debris with a larger average particle size. Variations in river discharge, which ranged between 0.31 and 2.91 m<sup>3</sup>/s, is the primary driver behind the diurnal SSC variability. Rising discharge is associated with a rise in SSC, which decreases at a slow rate, even though discharge is still high. Precipitation is the mechanism driving the large peaks in data. The availability of water, derived from rainfall and surface lowering on the glacier, allow the river to increase in velocity and thus erode larger amounts of sediment (figure 25). Each blue tick along the x-axis in Figure 25 represents 0.2mm of rainfall in a 30 minute increment. Dense concentrations of these ticks represent intense rainfall events on Linnèbreen (Figure 25 - 8/3, 8/5, 8/10). Days of intense precipitation and surface

lowering have profound influences on the discharge signal, characterized by the peak on 8/5 (figure 26). Temperature drove the diurnal variations in discharge; though precipitation allowed for high amplitude fluctuations (figure 26).

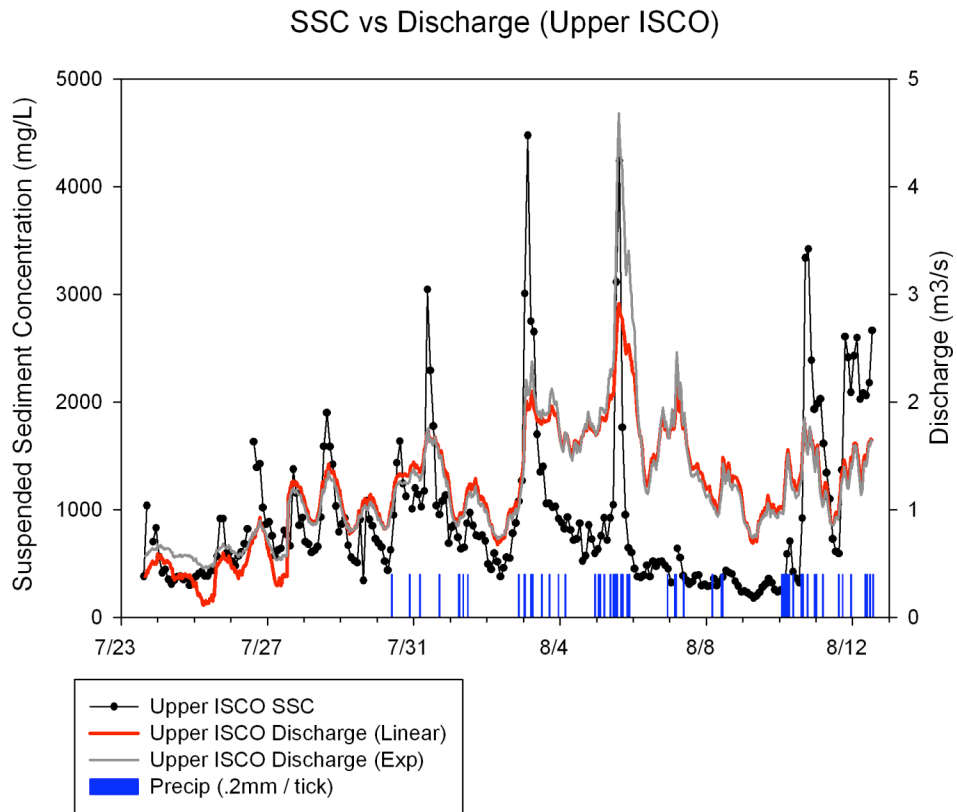


Figure 25: SSC, discharge, and precipitation correlations at the upper ISCO site

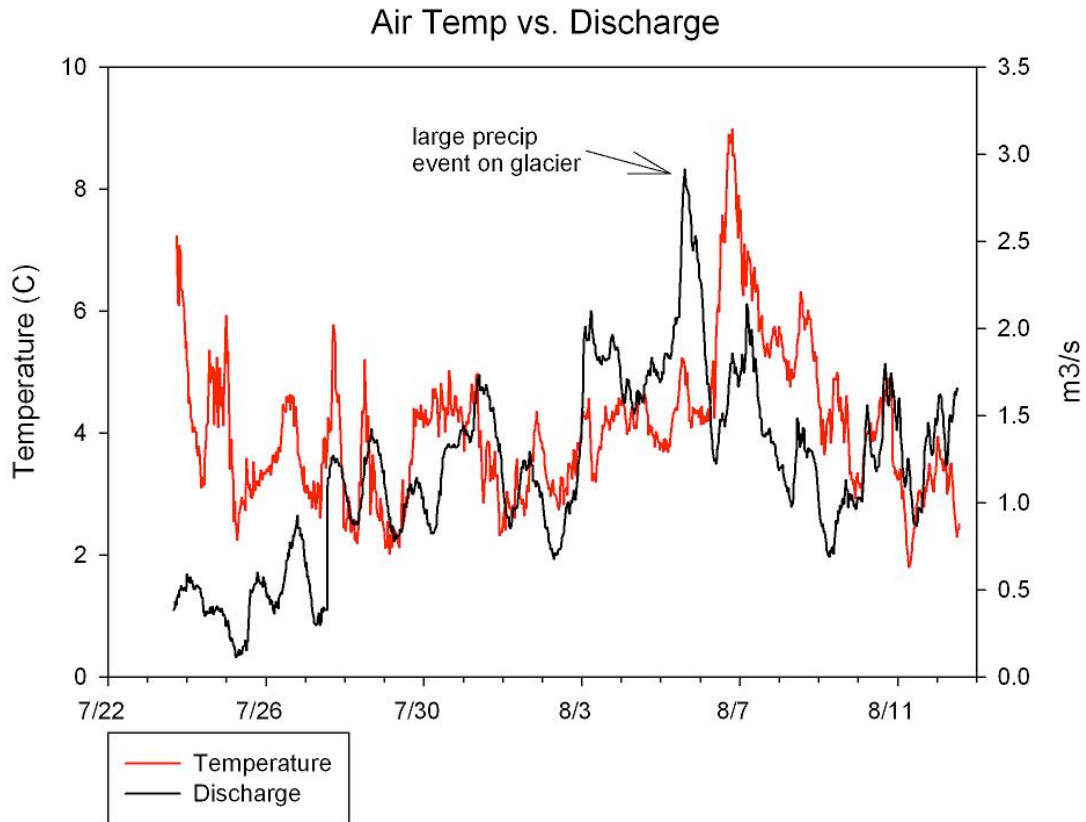


Figure 26: Diurnal discharge generally driven by temperature variations

The cumulative suspended sediment load was calculated by determining the sediment transport rate and integrating it with respect to time (Matell 2005). Each 2-hour SSC increment was multiplied by linearly extrapolated discharge values from the stage-discharge rating curve to create a total Suspended Sediment Load (SSL) graph (figure 27). 3121.9 metric tons of sediment was carried past the LIA moraine during our 21 day monitoring period (figure 27).

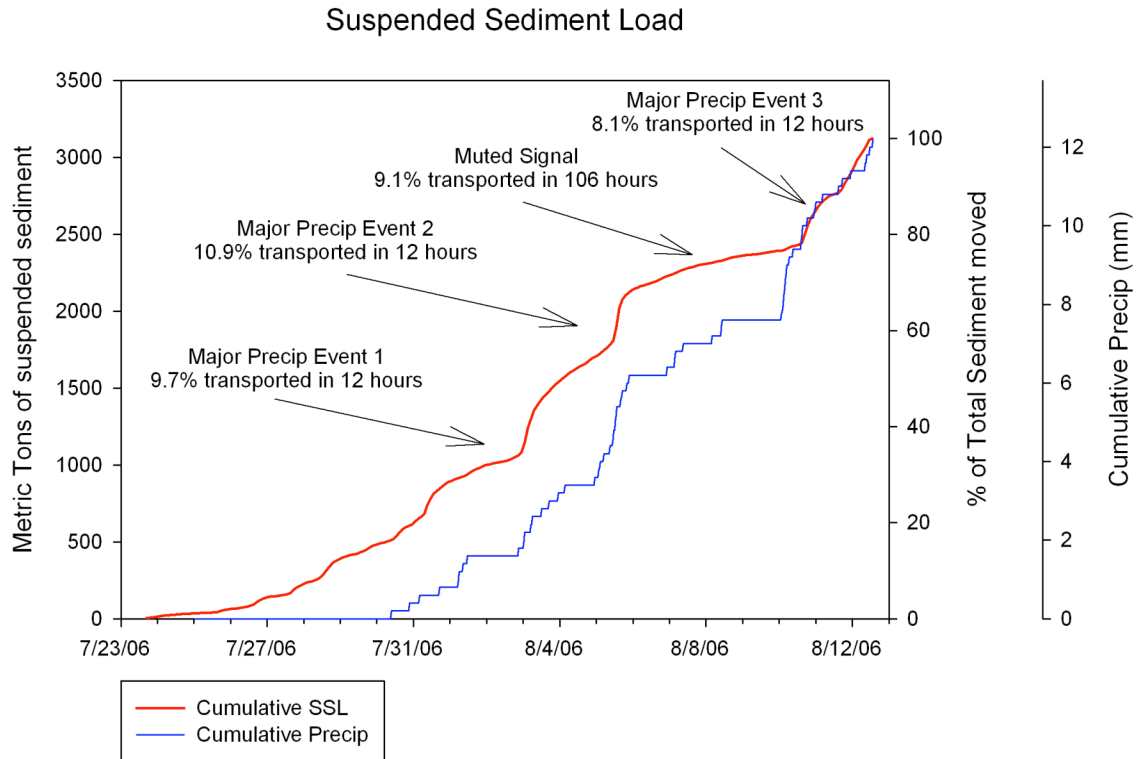


Figure 27: Cumulative sediment load computed from the upper ISCO site

To further explore this section of data, hysteresis curves were created to explore patterns in SSC vs. discharge during our field season. SSC vs. discharge was heavily influenced by precipitation (figure 25). Before the onset of the so-called muted SSC signal from 8/6/06-8/10/06, discharge and SSC follow the same rhythm from 7/23-8/5 (figure 27, 28). During this period, peak SSC occurred ~2 hours before peak discharge and the hysteresis plots illustrate a general clock-wise trend. This suggests a time of diurnal sediment flushing. Comparative discharges on the falling limb of the hydrograph have significantly less sediment concentrations than the previous rising. After 8/5, the hysteresis plots show peak SSC coming after peak discharge and exhibit a

counterclockwise trend. As seen in figure 25, after peak discharge on the 10<sup>th</sup> of August, SSC falls in concert with falling discharge. This decrease reflects a change from a supply-limited to transport limited movement system.

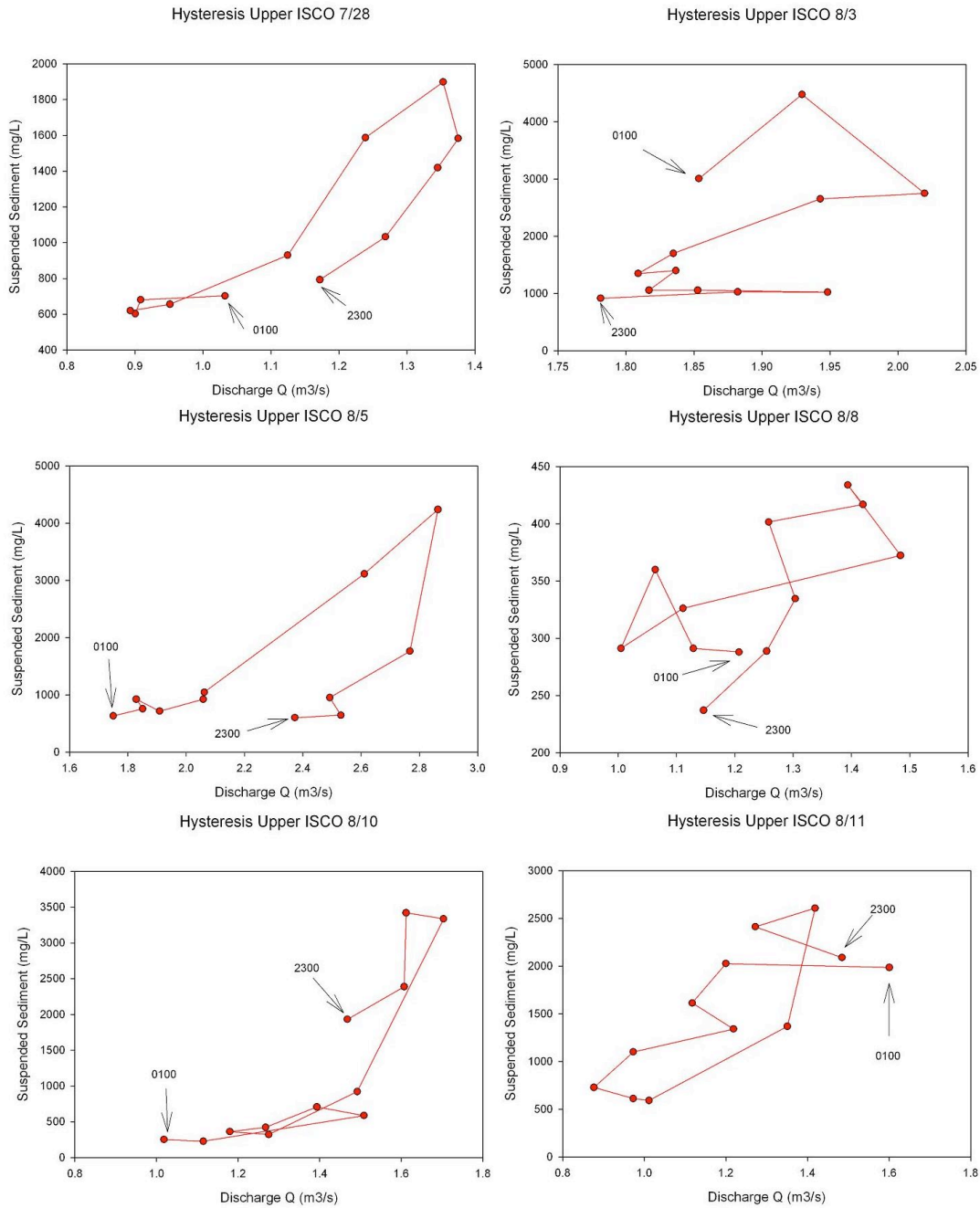


Figure 28: Hysteresis plots for the 2006 field season relating stream discharge to SSC over the meltseason

In order to determine sediment sources in the glacial environment, grab samples were also analyzed (figure 29, 30). Although lacking temporal resolution to properly characterize sediment flux off of the glacier, provides a basis for further study in subsequent years. During this period the glacier displayed two modes of sediment flux: one in which the higher sediment concentration was recorded down stream at the toe of the glacier in the main ice-marginal stream, and another when higher concentration was recorded after the mud flat. Samples were also taken from a large supraglacial channel near the headwall, this provided concentrations several magnitudes below the other sampling sites. All locations lie up valley of the LIA moraine and are unaffected by dilution from tributary streams into Linnèelva.

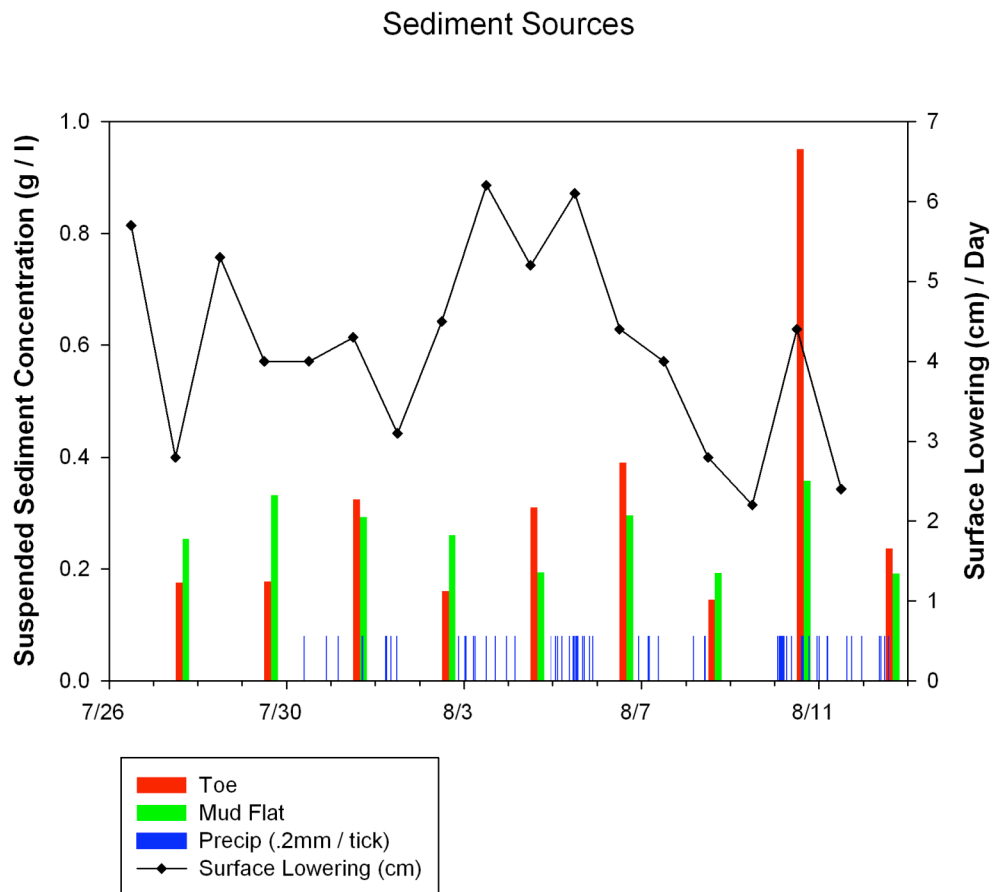


Figure 29: Grab sample analysis from Linnebreen

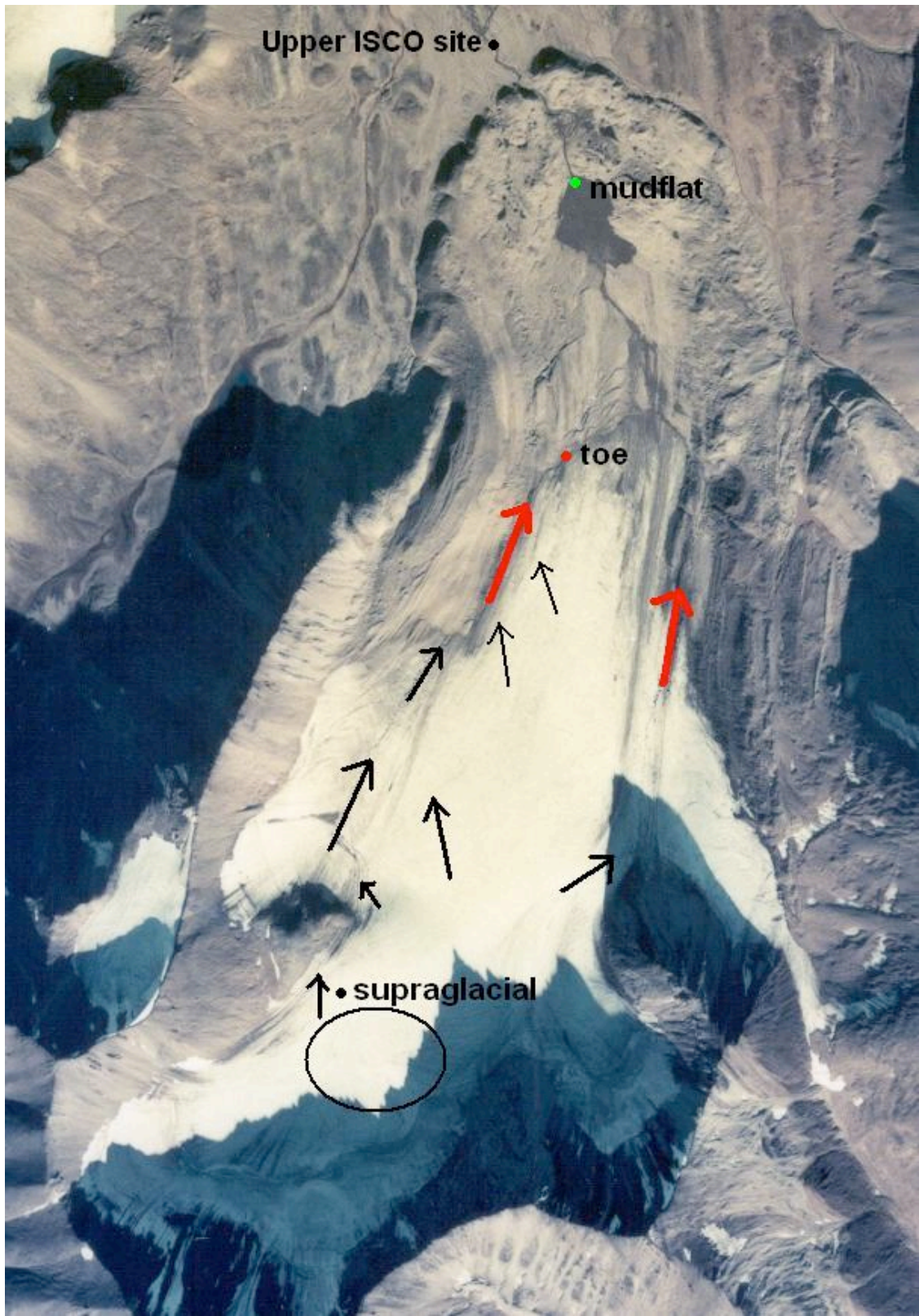


Figure 30: Vast supraglacial drainage networks on Linnébreen, black lines designate supraglacial flow, red lines designate ice marginal channels. Grab sample sites are noted by name and color

## 5) DISCUSSION

### *5.1 Examining Thermal Regimes*

Previous studies on the glacier lacked the temporal constraints to directly correlate meteorological fluctuations with glacier ablation. Surface lowering, measured every 2-4 days prior to 2006, was mainly attributed to variations in air temperature. These determinations, including the signals in fluvial and lacustrine environments, have all been based on the assumption that Linnèbreen is composed of warm-based ice. Svalbard's high-Arctic location and low mass balance gradient glacial environment contrast with those conducive of warm based glaciers (Hodgkins 1997). Pelto et al., 1990, demonstrates this by determining an average mass balance gradient of  $0.41\text{m } 100\text{m}^{-1}$  for eight Svalbard ice masses between  $78\text{-}79^\circ$  N latitude. This compares to  $0.86\text{m } 100\text{m}^{-1}$  for glaciers in Alaska,  $54\text{-}76^\circ$  N latitude, and  $1.24\text{m } 100\text{m}^{-1}$  for the North Cascade Range in Washington state,  $48\text{-}51^\circ$  N latitude (Pelto et al. 1990).

The thermal regime of an ice mass is a function of geothermal heat flux, air temperature, vertical and horizontal components of velocity, and basal friction (Hooke, 1998). Temperate glaciers are composed entirely of warm based ice, forming when ice is at the pressure melting point throughout. This condition arises from increased pressure associated with thick ice, high average air temperatures, and possibly high basal heat input (Menzies 2002). The basal layer of a large ice mass is under extremely high pressure, forcing the ice into its denser phase, water. The pressure melting point is derived from this fact, resulting in the lowering of melting temperature with increasing depth due to overlying pressure. Warm-based glaciers creep but also move through slip on the thin layer of water which lubricates their basal layer. Frictional contact generates

heat, resulting in an eventual increase in temperature with depth. Sliding glaciers erode basal sediment by a number of erosional processes which effectively act as a bulldozer, entraining and transporting debris to the terminus (Menziés 2002).

By contrast, cold based ice is entirely below the pressure melting point and frozen to its bed. Erosional landforms do not form in this type of environment as ice moves only through internal deformation (creep), an extremely slow process (Menziés 2002). Cold based ice also restricts meltwater percolation, which is transported off the glacier by a vast network of supraglacial and ice marginal channels (Hodgkins 1997). These ice masses can either be polar, entirely below the pressure melting point throughout, or subpolar, with frozen terminal zones but a warm based interior (Menziés 2002). Recent advances in glaciology acknowledge that many glaciers are, in fact, polythermal. This classification is divided between ice which is 1) warm based or cold based on a spatial scales of 1-10km and/or vary on a temporal scale of less than a decade; 2) now polar cold based but was once warm based; and 3) now warm based but once cold based (Menziés 2002).

The thermal regime of Linnébreen has not been properly determined. As noted before, Svendsen and Mangerud (1997) investigated cores from Linnèvatnet and interpreted Linnébreen's Holocene variations. They note that Linnébreen is considered to be subpolar in type, consistent with many glaciers on Svalbard (Svendsen and Mangerud 1997). Their interpretation of the lake cores suggest peak sedimentation and increased coal content during the LIA when Linnébreen was at its maximum extent (figure 9, 12). Svendsen and Mangerud (1997) attribute the increase in coal content to the basal entrainment of carboniferous sandstone which underlies Linnébreen. Provided the 40m

tall LIA moraine now lies ca. 1200m in front of Linnèbreen, it is possible that this glacier has significantly changed its thermal regime and sedimentation rate due to this dramatic loss of ice mass post LIA (figure 31,32).

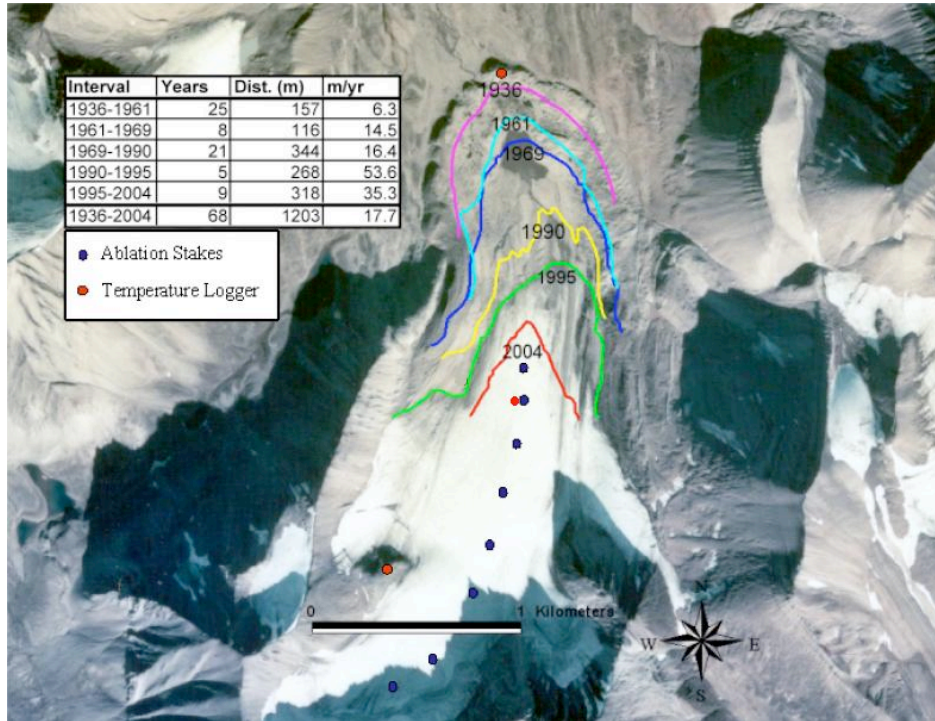


Figure 31: Air Photo / GPS recorded terminal extents and calculated retreat rate on Linnèbreen (Schiff 2004)



Figure 32: Linnèbreen during the 2006 field season

## *5.2 Ablation dynamics and sediment flux, a modern perspective*

Data collected during the 2006 modern process study of Linnèbreen, can be used to further examine glacier ablation, proglacial sedimentation signals, and provide a basis for understanding the glaciers thermal regime. Linnèbreen exists today as a small glacier which is entirely contained on a generally flat, uncrevassed surface from the terminus up to the cirque headwall (figure 32). During the 2006 field season, observations were taken of the entire glacial environment every other day. The surface of Linnèbreen consists of a vast supraglacial fluvial network, all draining into ice-marginal channels on either side of the glacier (figure 36, 38). At stake 7, near the cirque, a small depression and ponded meltwater was observed on the glaciers surface. The largest supraglacial stream on the glacier flows out of this depression and into the ice marginal channel on the western side of Linnèbreen (figure 36). Similar supraglacial lakes were observed by Liestøl et al. (1980) and Hagen et al. (1991) on Austre Broggerbreen, a glacier which is almost entirely cold based. This sign of restricted meltwater percolation, especially at the top of the glacier suggests the presence of cold-based ice.

During intervals of decreased precip and increased insolation, the ice surface of Linnèbreen has as a popcorn like texture. This is due to solar radiation and the buildup of eolian and supraglacially transported debris on the glaciers surface. Fresh debris melts in differentially due to contrasts in albedo, providing small melt pockets into the glaciers surface (figure 34, 35). A sampling of this surface ice gave a 50% porosity reading, representing the large amount of ice removed by albedo differences. This texture is removed after a large precipitation event, resulting in a glassy like surface texture. This transition is associated with precipitation, enhanced surface lowering, and sediment

release. Observations suggest Linnèbreen is now composed almost entirely of cold based ice. The extensive loss of mass and resultant post LIA thinning seems to have been enough to allow cold-based ice conditions to prevail. Enhanced surface lowering during precipitation events is outlined in figure 38. The addition of rainfall directly onto the surface of Linnèbreen allows sensible heat transfer to the ice surface and percolation into the “holes” created by the debris (figure 34, 35). This water subsequently refroze at the glaciers surface, releasing latent heat, and triggering the removal of overlying porous ice. As a result, the glacier surface became smooth and glassy surface after each precipitation event. Linnèbreen is thus re-defined today as a polythermal glacier due to its thermal regime change. Though once warm-based as outlined by Svendsen and Mangerud (1997), it now displays characteristics of cold-based ice. Thermal conditions, however, may vary on spatial/temporal scales.

Linnèbreen (LIN) compares well to Midre Lovenbreen (MLB) and Kongsvegen (KNG), similar glaciers along Spitsbergen’s west coast (figure 33). Both MLB and KNG are polythermal glaciers, though KNG contains a large volume of warm based ice due to its extensive size (Kohler – unpublished). There is documented supraglacial dominance of modern sedimentation on MLB due to its lack of bed modification (Glasser and Hambrey – unpublished). Structural mapping of the glacier shows folds, fractures, and entrained basal sediment, indicating the warm based nature of this glacier during the LIA max (Glasser and Hambrey- unpublished).

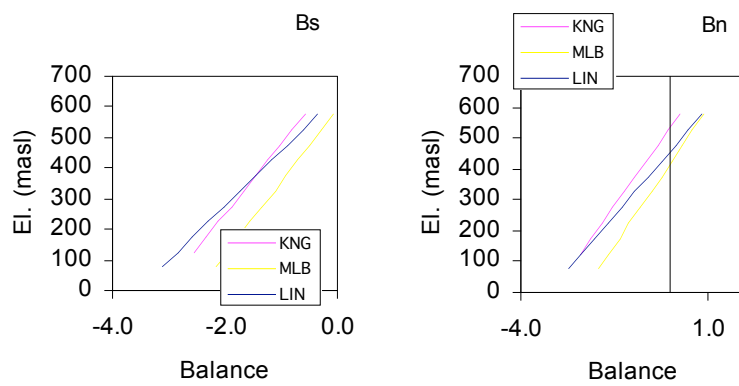


Fig 33: Summer and Net mass balances on similar Svalbard glaciers (Jack Kohler – email)



Figure 34: Popcorn surface texture, carpenters rule for scale



*Figure 35: Close up of popcorn surface texture*



*Figure 36: Large supraglacial stream which drains from the pool by stake 7*



*Figure 37: Supraglacial pool at stake 7*



*Figure 38: Ice-marginal channel on Linnèbreen's left lateral margin*

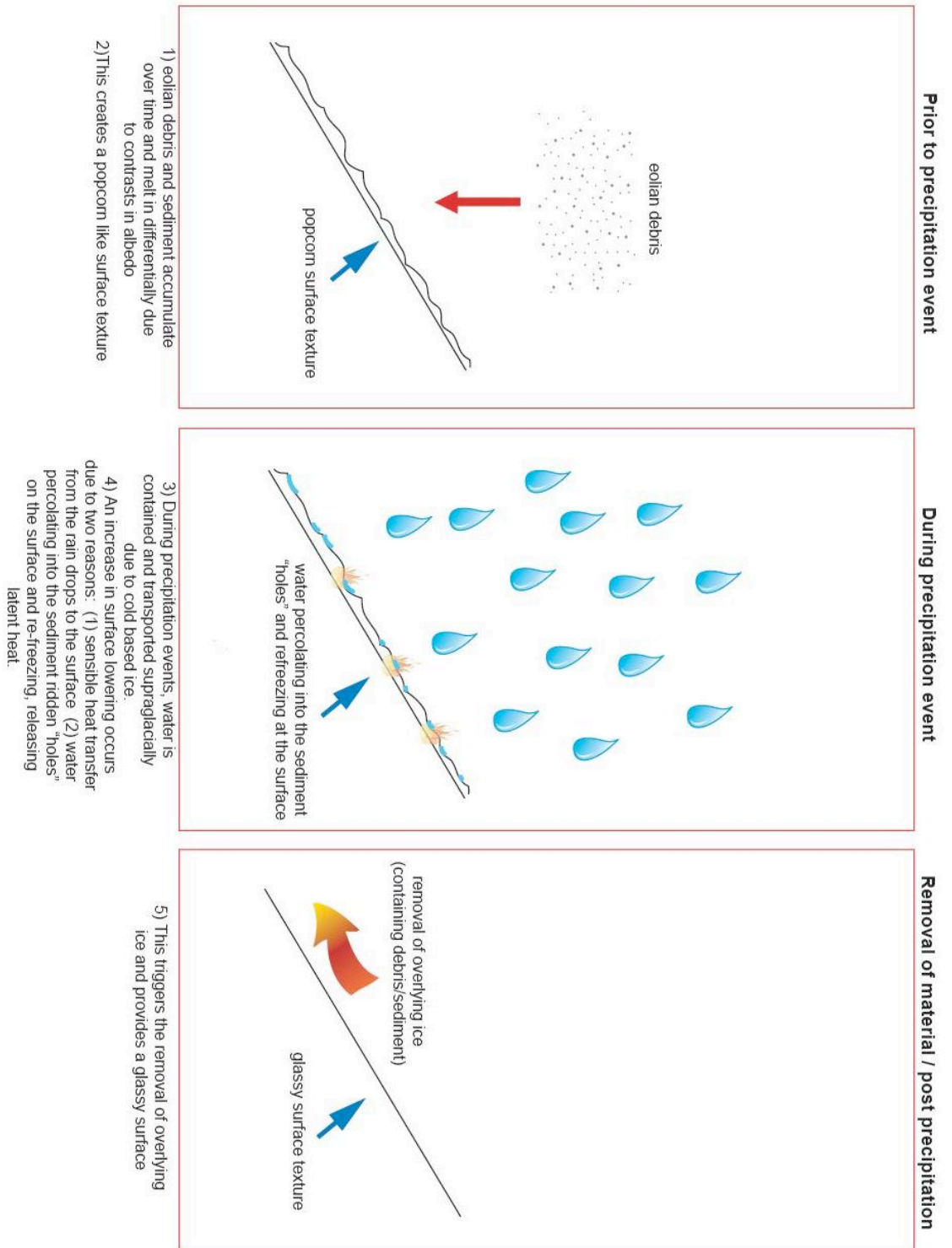


Figure 39: Graphical representation of precipitation induced surface lowering

Thermal regime change, thus causing a change in the hydrologic plumbing system of Linnèbreen, has a direct effect on sedimentation rates and “climate” signals in Linnédalen. Though there are no basal erosional processes, Hodgkins (1997) reiterates that drainage from cold based glaciers is not contained only in dilute supraglacial runoff. High energy fluvial environments have been documented on Scott Turnerbreen and Austre Broggerbreen due to supraglacial drainage and ice marginal streams, capable of entraining large amounts of ice marginal and proglacial sediment (Hodgkins 1997). These ice marginal channels present the possibility of temporary sediment storage when combined with diurnal discharge variations (figure 25). As discharge falls during the day, ice marginal channels store sediment as stream flow is no longer capable of transporting the particles in suspension. Lower discharge allows sediment storage in pools created in the channel during a high discharge / high volume event (Hodgkins 1997). The meltwater SSC supports these findings (figure 25). SSC concentrations increase abruptly as discharge grows and then fall quickly as discharge decreases on a diurnal timeframe, suggesting supply-limited transport, shown by the hysteresis plots (figure 25, 28). This storage is best represented by the high discharge/SSC event during 7/31 and subsequent rises during the 8/3 rainfall event. As discharge and subsequent ice marginal water volume increase again to their peak values on August 5<sup>th</sup>, additional sediment is liberated from the channels (figure 25). This event is connected to the large precipitation event recorded on that day. After this event Linnèlva appears to be operating in a sediment depleted mode, represented by the muted SSC signal from August 6<sup>th</sup>-9<sup>th</sup> (figure 25). This trend is only broken by large rainfall on August 10<sup>th</sup>.

Judging from the Grab samples taken over the meltseason, it appears that the bulk sediment is derived from ice marginal streams during times of precipitation induced high discharge and peak surface lowering (figure 29, 30). This can be attributed to the remobilization of coarser sediment that is temporarily stored in the ice marginal channels as discharge falls. Additions also come from the low SSC meltwater derived from the glacier surface. Surface lowering is a means of remobilizing debris previously entrained by the glacier. It is possible that a significant amount of the coarse sediment is lost to the mudflat due to a drop in stream velocity when it flows from a confined channel onto the open mudflat. During dry spells, especially in the early part of our field season, bulk sediment is derived from the mudflat due to stream erosion.

### *5.3 Sediment availability*

Roughly 30% of the total sediment was carried during three 12 hour periods, influenced by the major precipitation events on the glacier (figure 27). The muted SSC signal, which occurred from 8/6/06-8/9/06, resulted in only 9.1% of the cumulative load moved over this 106 hour period. By comparing this muted signal to the data recorded at the lower ISCO, we determined that these readings are not a result of instrumental error. Having followed the three peaks in discharge and SSC, this could be a period of sediment exhaustion in Linnédalen. This event occurred during the falling limb of total daily surface lowering after its two peaks on the 3<sup>rd</sup> and 5<sup>th</sup> of August. On 8/10, when the largest rainfall event of the field season occurred, sediment concentration rose almost by an order of magnitude in the latter portion of the day. Similar discharges at the falling end of the hydrograph carry much more sediment. This suggests that from 8/6-8/9 there was either a period of sediment storage on the glacier or complete exhaustion of the

system after the rain events on the 3<sup>rd</sup> and 5<sup>th</sup> of August. This is followed by rapid sediment saturation of the system on the 10<sup>th</sup>. The hysteresis plot from 8/8 shows SSC an order of magnitude lower than other plots, sequential with the extremely low sediment load carried during that time (figure 28).

Similar results have been observed in other Arctic locations. Lewis et al. (2005) ties a single 4 hour jökulhlaup event on Ellesmere Island, located in the Canadian High Arctic, to the movement of 32% of the cumulative SSL on July 7<sup>th</sup>-8<sup>th</sup> in 2004. This event was preceded by a long period of relatively high air temperature and was sparked by intense rainfall on July 7<sup>th</sup>. The muted SSC signal we see at Linnè, 8/6-8/9, follows two large rainfall events and peaks in SSC, discharge, and surface lowering (figure 22, 25). These events combine to exhaust the sediment supply to Linnèelva. On 8/6 both temperature and isolation reach their peak values on Linnèbreen (figure 22). The mean temperature on 8/6 was 9.8°C. 8/6-8/9 achieved a mean temperature of 5.5°C, well over the 4.07°C average for the 2006 field season on Linnèbreen (figure 20). August 10<sup>th</sup> marked the largest precipitation event on the glacier, totaling 4.6mm over the course of the day, comparable with the 5mm rain event noted by Lewis et al. (2005). This precipitation event along with added meltwater, noted by increased surface lowering on the glacier (figure 22), could trigger a mass wasting event such as slumping along the side of an ice marginal channel. The long period of high temperatures which preceded this could reflect a time of increased active layer thawing. The rain fall event on August 10<sup>th</sup> liberated this great abundance of material and Linnèelva thus moved into a transport limited mode at the upper ISCO site. This signal does not show up at the lower ISCO site

due to river storage of coarse particle material in the fluvial system (figure 40). Unfortunately, this event was not documented in the field.

After the August 10<sup>th</sup> event, there was an over abundance of sediment available for transport, indicative of the switch from supply limited to transport limited movement (figure 25, 28). The large sediment flux in the meltwater channel's grab sample concentration implies that this event occurred proximal to the lateral extent of Linnëbreen (figure 29,30). The importance of both high resolution SSC readings, and sediment availability derived from active layer thawing. This event would have been completely missed if the upper ISCO had been sampling over longer intervals, resulting in a gross underestimate of cumulative SSL transported during the 2006 melt season.

The 2005 field season recorded a muted diurnal SSC signal which represented the brief period of depletion in 2006 (figure 24, 40). Year 2005 recorded 5mm more precipitation than 2006, though this is not reflected in the SSC signal (figure 40, 41). Peaks in 2006 SSC data are directly connected to high discharge brought on by precipitation events (figure 25). Work by Matell (2005) found a significant relationship between grain size and discharge. By dividing the total SSL by the catchment's area, 6.75km<sup>2</sup> for the upper ISCO site, it is possible to calculate the total suspended sediment yield (Matell 2005). Over the 2006 field season the upper ISCO site yielded 462 t/km<sup>2</sup>. The 2005 calculation was limited to 8/1-8/10, yielding 244t/km<sup>2</sup> based on an averaged discharge [183 low – 326 high estimate] (Matell 2005). Our data allows for direct discharge correlation and yields 258 t/km<sup>2</sup> over this period in 2006. Based on SSC comparison graphs (figure 40), one can infer that the calculated yield using average 2005 discharge provides an overestimate due to low amplitude SSC variations.

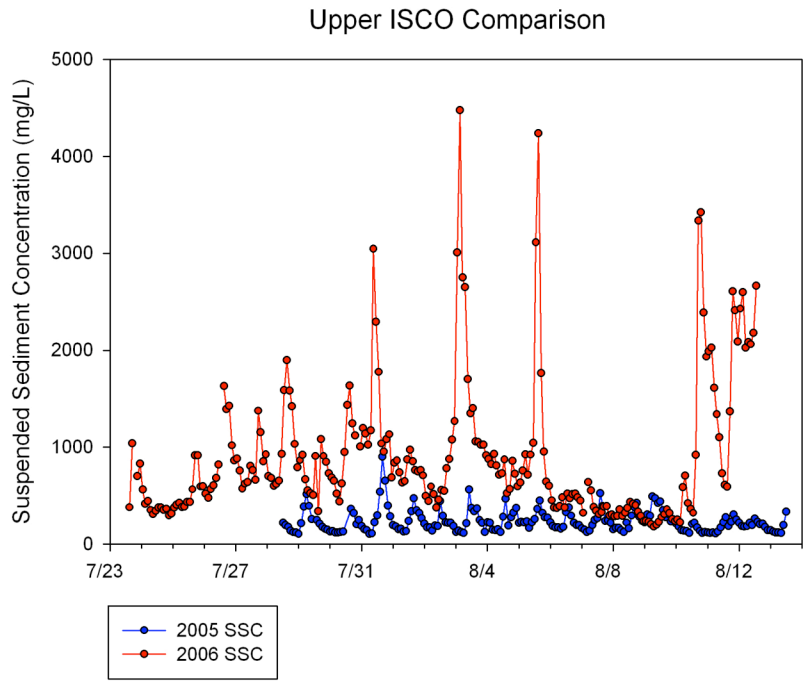


Figure 40: SSC comparison from 2006 and 2005 upper ISCO data

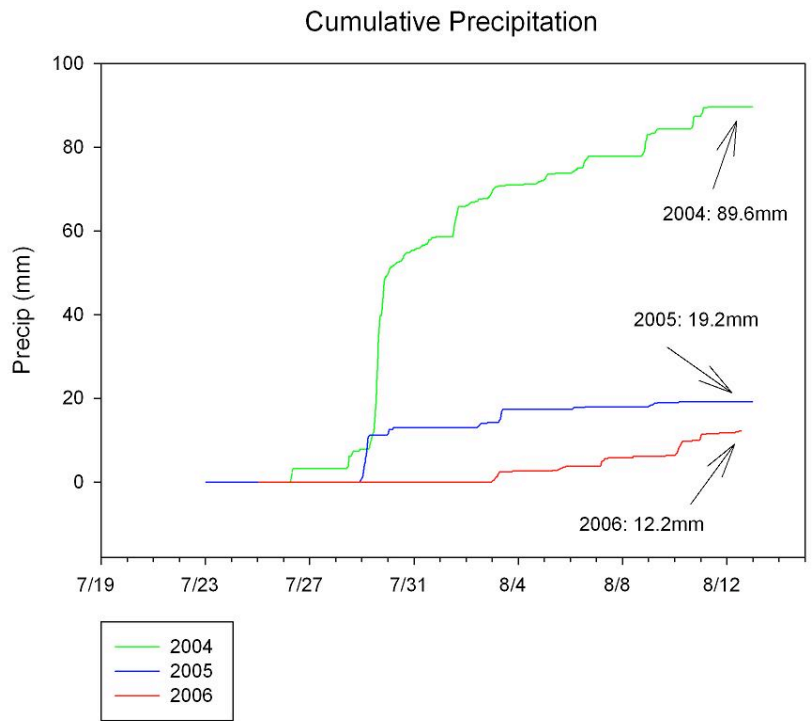


Figure 41: Precipitation comparison from the three field seasons

The recorded mean temperature in 2005 was 0.25°C below the 30 year average and 0.65°C below the past 10 year running mean (figure 44). Any link between the 2005 SSC plot and the 2006 depletion period (figure 40) could indicate that sediment was not readily available to the system during the 2005 field season. Abnormally low temps during the 2005 field season could also be a major contributor to the muted signal (figure 44). The rainy and warm 2004 field season yielded a sediment load which exceeds the 2006 data, representing the importance of air temperature and precipitation to the sediment signals and yield (figure 41, 44).

Based on sediment modeling by Matell (2005), a single rainfall event yielded 73.6% of the overall sediment load during the 2004 field season. There was a period, similar to 2006, of extremely high temperatures prior to this massive sediment flux of (figure 42). July 29<sup>th</sup> recorded a characteristically intense rainstorm which could have liberated the freshly thawed active layer sediment and carry it to Linnèvatnet. This event was recorded at the lower ISCO site just before Linnèvatnet, where as the 2006 event was recorded only at the upper ISCO site. The discrepancy may be tied either to the availability of sediment sources in 2004 or an extremely high discharge which allowed transport of coarser material in greater abundances. Discharges were inferred from stage data in 2004, similar in fashion to 2006. Results were one to two orders of magnitude greater than this year's data. This appears to be an overestimate derived from extrapolated data, but does present the notion that discharge was significantly higher on average in 2004. High discharges and sediment transport are linked to the tremendously high precipitation rate over this field season (figure 41, 43).

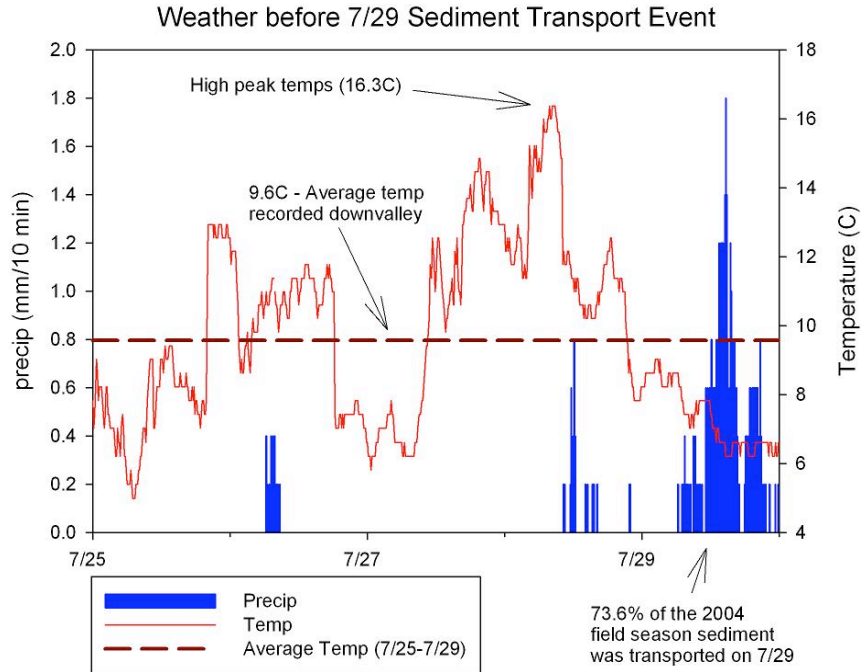


Figure 42: Weather record for the days leading up to the 7/29 sediment transfer event

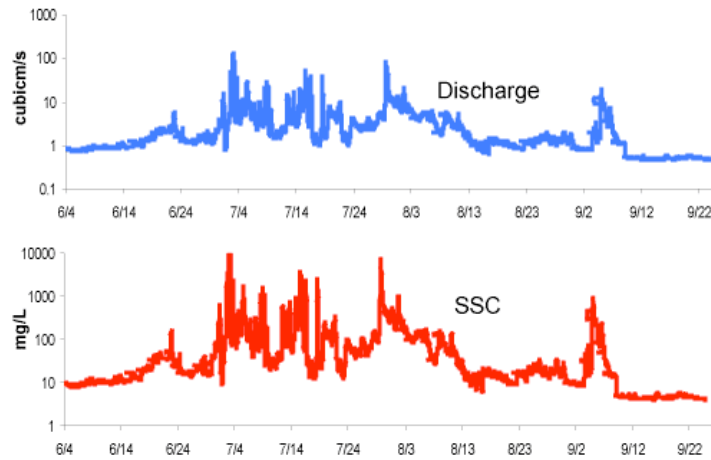


Figure 43: 2004 modeled SSC and discharge (Matell 2005)

Linnèbreen's cold based nature also suggests that fluvial processes dominate the denudation of this glacierized catchment. The trend from daily SSC lead to discharge lead on the hydrograph (figure 28) matches up with results from Hodgkins (1996) study on Scott Turnerbreen. Temperate conditions would produce contrasting results, as SSC and discharge can vary at the same pace for much of the meltseason (Hodgkins 1997). Based upon Linnèbreen's thermal regime, sediment is derived from fluvial erosion

instead of glacial. Sediment supply on the glacier is dominated by both active layer thawing, allowing entrainment of debris by fluvial means, and the liberation of previously entrained debris by surface lowering or terminus retreat. The rise and fall of SSC is directly connected to discharge and temporary storage in ice marginal channels / braidplains. In future melt seasons, without the extremely high temperatures and precipitation experienced in 2004, it is possible that Linnèelva will demonstrate further sediment depletion. The supply of sediment to the river also appears to be associated with the thickness of a seasonal active layer. This defines the “normal mode” of Linnèelva during the 2006 melt season as supply limited due to the lack of sediment provided by active glacial erosion. With high average temperatures and precipitation, such as the 2004 field season, rapid active layer thawing could deliver an over abundance of sediment and cause the conversion of Linnèelva to a transport limited mode.

The post LIA sedimentation drop, outlined by Svendsen and Mangerud (1997), may reflect a change in thermal regime at Linnèbreen. However, as rising temperatures continue in the Arctic summers, permafrost will continue to thaw at a rapid pace which will likely provide an increase in sediment for fluvial erosion. Sedimentation rates will likely increase in future studies at Linnèbreen, in response to warming in the Arctic (table 1). Circum-Arctic warming will deepen the active layer and degrade the permafrost which underlies over 85% of Arctic land (Alley et al. 2006). As outlined by Jansson et al. (2005), it is important to consider the entire system and mechanisms which provide sediment in order to make reliable interpretations from lacustrine sediment cores. Due to the mean annual 5°C warming after 1920 on Svalbard, linked to the termination of the

LIA, analysis of cores from Linnèvatnet should take into account the valley's changing mechanics.

<i>Period</i>	<i>Glaciation style</i>	<i>Linnèvatnet sedimentation rate [mm/yr] (Svendsen and Mangerud, 1997; Svendsen et al., 1989)</i>
13-10ka	Deglaciation	
Entire Holocene (10ka-present)	Variable	0.2
Early Holocene	Little	0.1 - 0.4
Late Holocene	Significant	1 - 7
Present (2004)	Deglaciation	1.6 (McKay, 2005)

Sedimentation rates are likely to rise as circum-arctic warming thaws the active layer  
Increases in the Arctic's precipitation budget will allow for more high discharge events

*Table 1: Sedimentation rates related to glacial activity (adapted from Matell 2005)*

#### *5.4 Thermal Regime Change at Linnèbreen and its implications for Svalbard*

By investigating the summer temperature over the last 30 years at Isfjord Radio, recent warming in Linnèdalen can be put in perspective (figure 44). Over this thirty year period, the running mean annual temperature is 4.9°C. Seven of the past ten years have exceeded this value. In fact, temperatures have risen by ~0.4°C over the past three decades. If this trend continues linearly, average temperatures could reach over 4°C warmer than the current thirty year average by the end of the century.

Thermal regime change and sedimentation reworking in Linnèdalen are key indications of rising temperatures. Recent work by Alley et al. (2006) cites climate model predictions of 4-6°C annual temperature rise in the Arctic by the end of the 21<sup>st</sup> century. Temperatures of this magnitude dwarf the 2°C warming experienced on Svalbard during the warm early Holocene, otherwise driven by orbital variations (Hald et

al. 2004). The average ELA on the archipelago was calculated at ca. 450m by Hagen et al. (2003), coinciding with the altitude containing the most ice mass. Further warming, changes in moisture advection, and a freshening of the Arctic Ocean are expected to cause a rise in the regional ELA. This will result in accelerated deglaciation of Svalbard, a situation unprecedented during the Holocene.

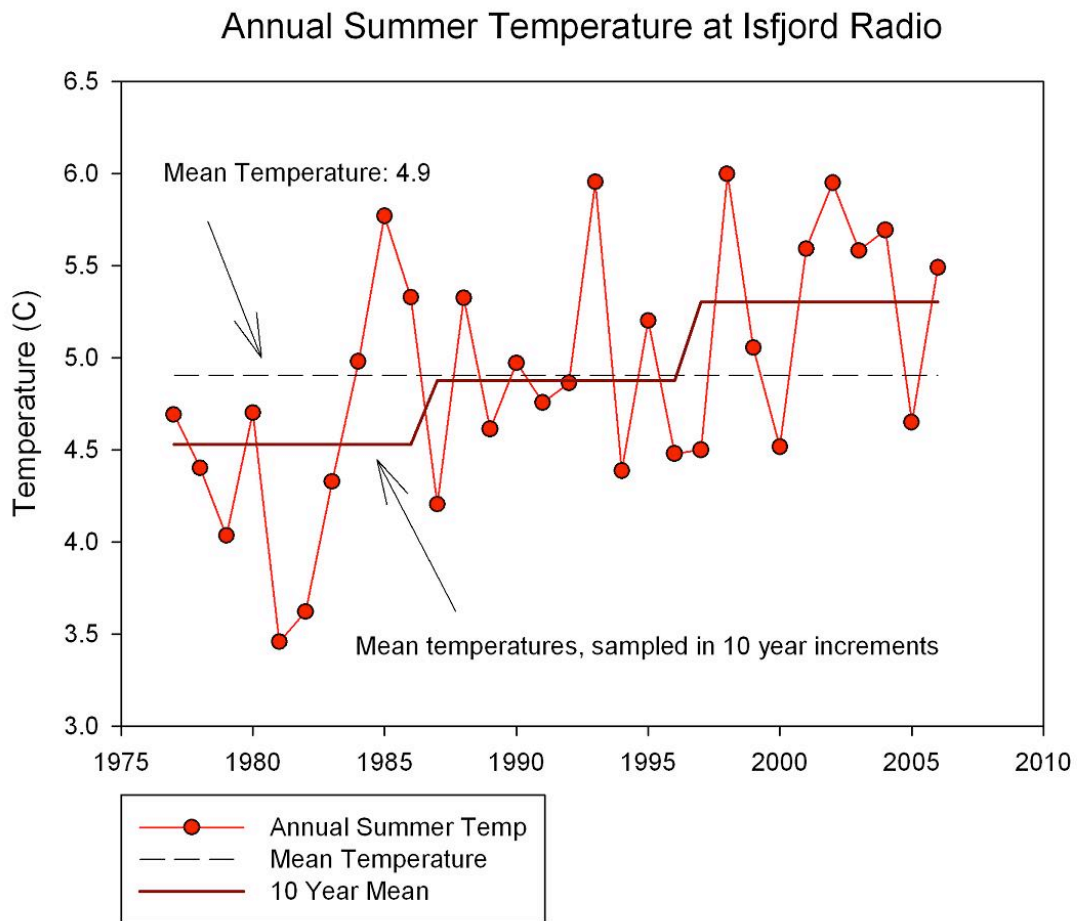


Figure 44: 30 year annual summer temperature comparison at Isfjord Radio

## 6) CONCLUSION

Post LIA and circum Arctic warming have had vast consequences on Svalbard. Resultant glacier thinning and terminus retreat, ca 1200m, from Linnèbreen's LIA max appears to have triggered a thermal regime change to cold based ice. Now a polythermal glacier, the main agent of surface lowering on Linnèbreen is summer precipitation, brought on by the sensible and latent heat flux of refreezing precipitation/meltwater. Sediment flux into Linnèelva is derived by fluvial means from sediment glacially eroded sediment. Supply is dominated by active layer thawing, resulting from rising temperatures and precipitation-induced high discharge. The rise and fall of discharge, allowing temporary storage in ice-marginal channels and braidplains, display a diurnal SSC trend. Linnèelva operates dominantly in a supply-limited mode due to the lack of active glacial erosion, with signs of sediment depletion over the meltseason. Sedimentation rates are likely to rise in coming years as the active layer seasonally deepens due to rising temperatures; proposed increases in the Arctic's precipitation budget allow for high discharge events.

Climate model predictions, outlined by Alley et al. (2006), show a 4-6° C warming in the Arctic by the end of the 21<sup>st</sup> century. Svalbard is in danger of unprecedented Holocene deglaciation due to the abundance of ice mass near the mean ELA. Temperatures well over those estimated for the early Holocene will result in a regional ELA rise, further degradation of Svalbard's ice masses, and widespread active layer thawing. Processes in Linnèdalen exhibit tell-tale signs of these modifications. Glacial activity, sediment transport, and lacustrine deposition in Linnèdalen must be evaluated in the future with respect to these changing mechanics.

## 7) FURTHER RESEARCH

In order to properly characterize this glacier, additional techniques are necessary to fully understand Linnèbreen's dynamics. Glacier surface texture has a profound effect on ablation dynamics. To properly connect changes in surface texture to increased surface lowering, I suggest setting up an automated time-lapse camera on the snow sensor's frame. These instruments can be programmed to take concurrent readings, allowing classification for each data point recorded by the snow sensor. Time lapse photography is also needed to define the supraglacial pool's role in Linnèbreen's dynamics (figure 37). Photography allows classification of its changing shape, size, and texture over time, allowing quantification of meltwater storage and release cycles. Additional ISCO automatic water samplers are required to narrow down sediment flux off the glacier. I suggest we setup one in the prominent ice marginal channel along the western margin of Linnèbreen, and one just before the stream runs through the mudflat and drops down the LIA moraine. This setup allows proper examination of the proglacial system, defining areas of fluvial sediment entrainment in relation to external meteorological influences and glacier behavior.

Where my data presents direction when trying to interpret Linnèbreen's thermal regime, proper instrumental investigation is essential. The glacier's thermal stratification can be investigated through borehole temperature measurements. This method allows us to determine the current thickness of Linnèbreen and temperatures reached at the basal layer. Ground penetrating radar (GPR) allows proper classification of a glaciers thermal regime. Results from GPR allow investigation into englacial/subglacier environments and the transition to warm based ice, if present in Linnèbreen's structure.

## **ACKNOWLEDGEMENTS**

Special thanks to:

NSF and UNIS

**Mentors:** Al Werner, Mike Retelle, Steve Roof, and Julie Brigham-Grette.

**2006 Svalbard REU participants:** Maggie Kane, Caroline Alden, Leif Anderson, Christina Carr, Bennet Leon, Heidi Roop, Ben Schupack, and Heather Stewart

**Logistics / miscellaneous:** Jorgen Haagensli, Hanne Christiansen, Jack Kohler, our cooks (Mark, Metta, and Mort), Karolina, Nuna, Silva

I would also like to recognize the unbelievable dedication displayed by Sheila Seaman, Mark Leckie, Mike Williams, Ray Bradley, and the UMASS Geosciences department

Skol!

## Works Cited

- Alley, R., Brigham-Grette, J., Polyak, L., Miller, G., 2006, Prospectus for Synthesis and Assessment Product 1.2 – Past Climate Variability and Change in the Arctic and at High Latitudes, *Draft*
- Bogen, J., 1991, Erosion and sediment transport in Svalbard, *Arctic Hydrology – Norwegian National Committee for Hydrology*, 121-131
- Boyum, A., Kjensmo, J., 1978, Physiography of Lake Linnevatn, western Spitsbergen, *Vehr. Internat. Verein. Limnol.*, 20, 609-614
- Carr, C., 2006, Suspended Sediment Transport in Proglacial Linnèelva, Spitsbergen, *unpublished undergraduate thesis – Montana State University*
- Glasser, N.F., Hambrey, M.J., Structural Evolution of a Polythermal Glacier (Midre Lovenbreen, University of Wales, Aberystwyth - unpublished work
- Grecke, E., 2006, Relationships among Weather, Glacial Ablation, and Flubial Processes, Svalbard, Norway, unpublished undergraduate thesis – *College of William and Mary*
- Hassol, S., 2004, Arctic Climate Impact Assessment, 2004, *Cambridge University Press*
- Hagen, J., Melvold, K., Pinglot, F., Dowdeswell, J.A., 2003, On the Net Mass Balance of the Glaciers and Ice Caps in Svalbard, Norwegian Arctic, *Arctic , Antarctic, and Alpine Research*, 35, 2, 264-270
- Hagen, J., Saetrang, A., 1991, Radio-echo soundings of sub-polar glaciers with low-frequency radar, *Polar Research* , 9, 99-107
- Hald, M., Ebbesen, H., Forwick, M., Godtlielsen, F., Khomenko, L., Korsun, S., Olsen, L., Vorren, T., 2004, Holocene paleoceanography and glacial history of the West Spitsbergen area, Euro-Arctic margin, *Quaternary Science Reviews*, 2075-2088
- Hodgkins, R., 1996, Seasonal trends in suspended-sediment transport at an Arctic glacier, and their implications for drainage system structure. *Annals of Glaciology*, 22, 147-151
- Hodgkins, R., 1997, Glacier Hydrology in Svalbard, Norwegian High Arctic, *Quaternary Science Reviews*, 16, 957-973
- Hodson, A., 1994, Climate, Hydrology, and Sediment transfer process interaction in a sub-polar glacier basin, Svalbard, *Unpublished Ph.D. Thesis – University of Southampton*

- Hook, R., Le, B., Gould, J., Brozowski, J., 1983, Near-surface temperatures near and below the equilibrium line on polar and subpolar glaciers, *Zeitschrift Fur Gletschekunde und Glazialgeologie*, 19, 1-25
- Humlum, O., 2002, Modelling late 20<sup>th</sup>-century precipitation in Nordenskiöld Land, Svalbard, by geomorphic means, *Norwegian Journal of Geography*, 56, 96-103
- Intergovernmental Panel on Climate Change, 2007, *Climate Change 2007: The Physical Science Basis- Summary for Policymakers*
- Jansson, P., Rosqvist, G., Schneider, T., 2005, Glacier fluctuations, suspended sediment flux and glacio-lacustrine sediments, *Georg. Ann.*, 87 A(1), 37-50
- Kohler, J., NP Mass Balance Measurements of Glaciers in Svalbard, Norwegian Polar Institute – unpublished work
- Lewis, T., Braun, C., Hardy, D., Francus, P., Bradley, R., 2005, An Extreme Sediment Transfer Event in a Canadian High Arctic Stream, *Arctic, Antarctic, and Alpine Research*, 37-4, 477-482
- Liestøl, O., Repp, K., Wold, B., 1980, Supraglacial lakes in Spitsbergen, *Norsk Geografisk Tidsskrift*, 24, 89-92
- Matell, N., 2005, The role of the valley braidplain as a sediment sink: Linnødalen, Svalbard, *unpublished undergraduate thesis- Williams College*
- Mangerud, J., Dokken, T., Hebbeln, D., Heggen, B., Ingolfsson, O., Landvik, J. Y., Mejahl, V., Svendsen, J. I., Vorren, T. O., 1998, Fluctuations of the Svalbard-Barents Sea Ice Sheet During the Last 150,000 Years, *Quaternary Science Reviews*, 17, 11-42
- Menzies, J., 2002, *Modern and Past Glacial Environments, Butterworth-Heinemann*
- Overpeck, J., Hughen, K., Hardy, D., Bradley, R., Case, R., Douglas, M., Finney, B., Gajewski, K., Jacoby, G., Jennings, A., Lamoureux, S., Lasca, A., MacDonald, G., Moore, J., Retelle, M., Smith, S., Wolfe, A., Zielinski, G., 1997, Arctic Environmental Change of the Last Four Centuries, *Science*, 278, 1251-1256
- Pelto, M., Higgins, S., Hughes, T., Fastook, J., 1990, Modeling mass-balance changes during a glaciation cycle, *Annals of Glaciology*, 14, 238-241
- Repp, K., 1988, The hydrology of Bayelva, Spitsbergen, *Nordic Hydrology*, 19, 259-268
- Serreze, M., Barry, R., 2005, *The Arctic Climate System, Cambridge University Press*
- Svendsen, J., Mangerud, J., Miller, G., 1989, Denudation rates in the Arctic estimated

- from lake sediments of Spitsbergen, Svalbard, *Palaeogeography*, 76, 153-168
- Svendsen, J., Mangerud, J., 1997, Holocene glacial and climatic variations on Spitsbrgen, Svalbard, *The Holocene*, 7.1, 45-57
- Vane, G., Etzelmuller, B., Odegard, R., Sollid, J., 1996, Meltwater routing in high arctic glacier, Hannabreen, northern Spitsbergen, *Norsk Geografisk Tidsskrift*, 50, 67-74